JOC The Journal of Organic Chemistry

Article

pubs.acs.org/joc

Selective Transition State Stabilization via Hyperconjugative and Conjugative Assistance: Stereoelectronic Concept for Copper-Free Click Chemistry

Brian Gold, Nikolay E. Shevchenko, Natalie Bonus, Gregory B. Dudley, and Igor V. Alabugin*

Department of Chemistry and Biochemistry, Florida State University, Tallahassee, Florida, 32306-4390

Supporting Information

ABSTRACT: Dissection of stereoelectronic effects in the transition states (TSs) for noncatalyzed azide−alkyne cycloadditions suggests two approaches to selective transition state stabilization in this reaction. First, the formation of both 1,4- and 1,5-isomers is facilitated via hyperconjugative assistance to alkyne bending and C···N bond formation provided by antiperiplanar σ-acceptors at the propargylic carbons. In addition, the 1,5-TS can be stabilized via attractive C−H···F interactions. Although the two effects cannot stabilize the same transition state for the cycloaddition to α,α-difluorocyclooctyne (DIFO), they can act in a complementary, rather than competing, fashion in acyclic alkynes where B3LYP calculations predict up to ∼1 million-fold rate increase relative to 2-butyne. This analysis of stereoelectronic effects is complemented by the distortion analysis, which provides another clear evidence of selective TS stabilization. Changes in electrostatic potential along the reaction path revealed that azide polarization may create unfavorable electrostatic interactions (i.e., for the 1,5-regioisomer formation from 1-fluoro-2-butyne and methyl azide). This observation suggests that more reactive azides can be designed via manipulation of charge distribution in the azide moiety. Combination of these effects with the other activation strategies should lead to the rational design of robust acyclic and cyclic alkyne reagents for fast and tunable "click chemistry". Further computational and experimental studies confirmed the generality of the above accelerating effects and compared them with the conjugative TS stabilization by π-acceptors.

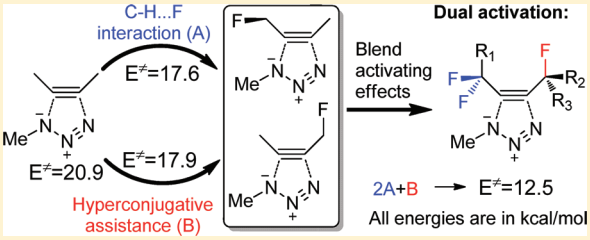

INTRODUCTION

"Click chemistry",[1] organic coupling reactions that meet a series of strict criteria for coupling efficiency, finds numerous applications in fields ranging from drug design[2] and chemical biology[3] to materials science,[4] development of sensors,[5] and polymer chemistry.[6] The copper-catalyzed azide−alkyne cycloaddition (CuAAC),[7,8] a variant of the Huisgen[9] 1,3-dipolar cycloaddition, has emerged as the prototypical example of a "click reaction".[10] This process is fast, insensitive to changes in solvent and/or pH, tolerant of a broad range of functionality and produces no byproduct. However, it does require a catalyst, namely, a copper salt, and the toxicity of copper salts limits *in vivo* applications of CuAAC couplings.[11] A click reaction that satisfies all of the above criteria without the need for a catalyst would be ideal.

Inspired by the "explosive" reactivity of cyclooctyne (OCT) toward organoazides,[12] Bertozzi,[13] Boons,[14] and others[15] are developing strain-promoted azide−alkyne cycloadditions (SPAAC) as a catalyst-free alternative to the CuAAC with reactivity suitable for a variety of applications.[16,17] For example, Bertozzi and co-workers demonstrated that intracellular azide-cyclooctyne coupling occurs within hours at room temperature[18] and enables *in vivo* biological imaging.[19] Boons introduced dibenzocyclooctyne (DIBO) reagents,[12] where further reactivity enhancements over cyclooctyne are achieved as a result of an increase in ring strain (more sp^2-centers). In an effort to "brush against the line between stability and reactivity without crossing it", Bertozzi reported that lactam-based BARAC (Figure 1) provides a 10-fold increase in reactivity over DIBO, leading to intracellular coupling within minutes.[20] The drawback, however, is that the reagent (and its derivatives) "should be stored as a solid at 0° C protected from light and oxygen."

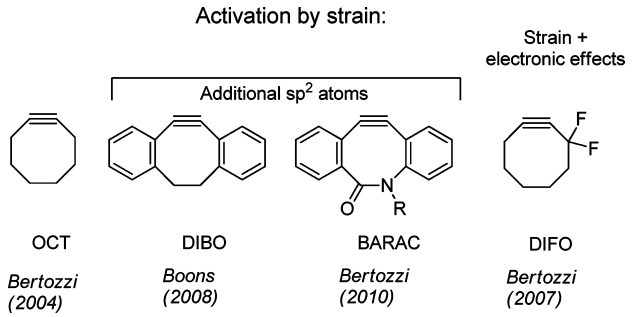

Figure 1. Literature approaches to alkynes with increased reactivity in noncatalyzed cycloaddition with azides.

Received: July 11, 2011
Published: November 11, 2011

   dx.doi.org/10.1021/jo201434w | J. Org. Chem. 2012, 77, 75−89

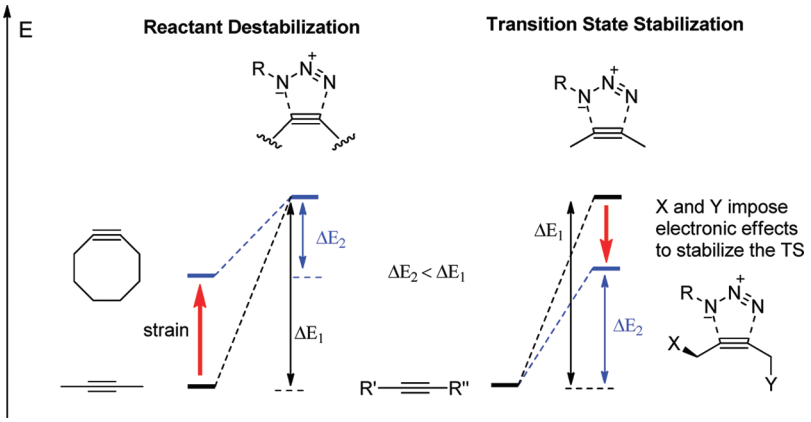

Figure 2. Comparison of strategies for acceleration of copper-free click reactions.

This decrease in stability is typical for reagents activated via reactant destabilization. The low stability of BARAC suggests that this approach gets close to the limit for its practical utility. In order to activate alkynes toward click chemistry without sacrificing their stability or compromising functional group tolerance, one has to decrease TS energy, either by minimizing unfavorable interactions[21] or by maximizing stabilizing effects in the TS (Figure 2). Selective TS stabilization is particularly attractive if the fine "line between stability and reactivity"[20] in the design of robust, yet reactive, alkynes is to be broadened. In this context, an interesting observation by Bertozzi et al. was that reactivity of OCT can be enhanced >50-fold by incorporation of electronegative fluorine atoms at the propargylic position (cf. DIFO). Houk and co-workers have shown that the ~2 kcal/mol decrease in the activation barrier for DIFO relative to cyclooctyne is reproduced by DFT computations.[22] This decrease has been attributed to LUMO lowering, but more specific orbital effects were not identified.

Since the donor ability of chemical bonds increases upon their distortion, the interaction with a properly positioned acceptor moiety should increase as bending increases, such as is the case in the highly bent cycloaddition TS. The greater distortion in the TS should lead to an increase in this stabilizing interaction, thus providing an approach to selective TS stabilization.

Our previous research in stereoelectronic effects[23] and alkyne chemistry[24,25] suggested to us that the accelerating effect of vicinal fluorines may stem from the increase in hyperconjugative interaction between the alkyne π-system and vicinal σ^*_{C-F} acceptors. This effect would be similar to the electronic origin of torquoselectivity in electrocyclic reactions,[26] where hyperconjugative interactions provide selective stabilization to the TS because of the increased donor and acceptor ability of chemical bonds upon their distortion and breaking.

As a first step, we have investigated the possibility of selective stabilization of bent alkynes via stereoelectronic hyperconjugative interactions with appropriately positioned σ-acceptors. In this part, we use DFT calculations in conjunction with natural bond orbital (NBO) analysis for dissecting the key electronic components responsible for the enhanced reactivity of DIFO relative to cyclooctyne. In the second part, we test conclusions derived from this analysis by analyzing stereoelectronic effects of propargylic fluorines on alkyne bending and reactivity in click cycloadditions. After identifying the most efficient patterns, we illustrate how fully compatible accelerating approaches can be combined toward the design of highly reactive and tunable alkyne substrates for click chemistry. In the final part, we combine experiments and computations to compare the importance of accelerating effects identified in this work with conjugative assistance to cycloaddition imposed by a π-acceptor. Because this study focuses on transition-state stabilization rather than reactant destabilization, it offers a possibility of selective acceleration of azide−alkyne cycloadditions without compromising reactant stability.

COMPUTATIONAL DETAILS

The computational analysis of potential energy profiles for azide−alkyne cycloadditions is performed at the B3LYP/6-31G(d) and B3LYP/6-31G(d,p) levels of theory. For 1,3-dipolar cycloadditions, B3LYP/6-31G(d) and B3LYP/6-31+G(d,p) have mean absolute deviation of 1.5 and 2.6 kcal/mol, respectively, relative to the highly accurate multicomponent CBS-QB3 method for activation barriers.[27]

Frequency calculations were performed to confirm each stationary point as minima or first-order saddle points. Free energies of activation and reaction have been calculated and are given in the Supporting Information. Solvation corrections were performed on the gas phase geometries at the B3LYP/6-31G(d) level of theory. A CPCM dielectric continuum solvent model for acetonitrile and water with UA0 radii was used before for related cycloadditions by Houk and co-workers.[34] This model does not explicitly include nonelectrostatic contributions, cavitation, and dispersion energies and should be considered as the first approximation of solvation effects.[28]

Electronic structures of reactants and transition states were analyzed using NBO analysis. The NBO 4.0[29] program was used to evaluate the energies of hyperconjugative interactions. The NBO analysis transforms the canonical delocalized Hartree−Fock (HF) MOs or corresponding natural orbitals of a correlated description into localized orbitals that are closely tied to chemical bonding concepts. Filled NBOs describe the hypothetical strictly localized Lewis structure. The interactions between filled and vacant orbitals represent the deviation of the molecule from the Lewis structure and can be used as a measure of delocalization. This method gives energies of hyperconjugative interactions both by deletion of the off-diagonal Fock matrix elements between the interacting orbitals and from the second order perturbation approach:

$$E(2) = -n_\sigma \frac{\langle \sigma/F/\sigma^* \rangle^2}{\varepsilon_{\sigma^*} - \varepsilon_\sigma} = -n_\sigma \frac{F_{ij}^2}{\Delta E} \quad (1)$$

where $<\sigma/F/\sigma^*>$, or F_{ij} is the Fock matrix element between the i and j NBO orbitals, ε_σ and ε_σ* are the energies of σ and σ^* NBOs, and n_σ is the population of the donor σ orbital.[30,31] Detailed descriptions of the NBO calculations are available in the literature.[32,33]

dx.doi.org/10.1021/jo201434w | J. Org. Chem. 2012, 77, 75−89

RESULTS AND DISCUSSION

OCT versus DIFO: Dissection of Hyperconjugative Contributions to the Activation Barrier. The cycloaddition of α,α-difluorosubstituted cyclooctyne synthesized by Bertozzi and co-workers has been previously investigated computationally by Houk[34] and Goddard,[21] who found that addition of fluorine substituents in the propargylic position lowered the free energy of activation for 1,5-addition by ~2 kcal/mol. Our calculated free energies of activation of 22.2 and 20.2 kcal/mol for the addition of methyl azide to cyclooctyne and 3,3-difluorocyclooctyne at the B3LYP/6-31G(d) level of theory are in good agreement with the literature data.

Quantifying hyperconjugative effects via NBO analysis revealed that hyperconjugative donation from the in-plane alkyne π-system to the σ^*_{C-F} orbital directly leads to the TS stabilization and explains the increased reactivity of DIFO compared to OCT (Figure 3). This interaction increases by

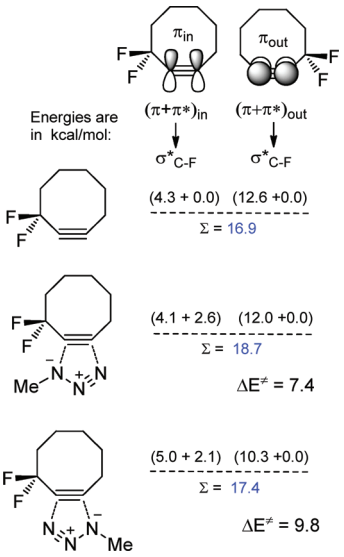

Figure 3. Hyperconjugative interactions between σ^*_{C-F} acceptor and the two π-systems in DIFO and two regioisomeric TSs for its cycloaddition to methyl azide. The data are for NBO second order perturbation energies in kcal/mol at the B3LYP/6-31G(d) level. $\Delta E^{\ddagger}$ values at the same level of theory are given at the bottom.

2.8 kcal/mol (from 4.3 to 7.1 kcal/mol, a ~65% increase) when the alkyne is distorted from the reactant to the TS geometry. Intriguingly, the magnitude of this increase matches well with the 2 kcal/mol decrease in the overall activation barrier.

These observations are especially interesting because the exocyclic C−F bonds are not fully aligned with the breaking in-plane π-bond (as illustrated by the greater energies of $\pi_{out} \rightarrow \sigma^*_{C-F}$ interactions in Figure 3), and one could expect that the TS-stabilizing effect to be enhanced once such alignment is achieved. Basic stereoelectronic expectations suggest that the $\pi \rightarrow \sigma^*_{C-X}$ interaction will be maximized for the antiperiplanar orbital arrangement.[35]

Testing the Hyperconjugative Model: 2-Butyne versus 1-Fluoro-2-butyne. In order to test the above stereoelectronic expectations, we have investigated conformational effects on the distortion and reactivity of 1-fluoro-2-butyne.

Effect of Propargylic Acceptors on Alkyne Bending. If the donor ability of alkynes increases upon its bending, one should expect that the magnitude of hyperconjugative interaction with an appropriately positioned σ-acceptor would increase as the alkyne moiety deviates from linearity. Such an increase in the stabilizing interaction should partially offset the energy cost for distortion. Indeed, we have found that the energy penalty for symmetric bending of 1-fluoro-2-butyne is lower than it is for 2-butyne (Figure 4). The hyperconjugative origin of this

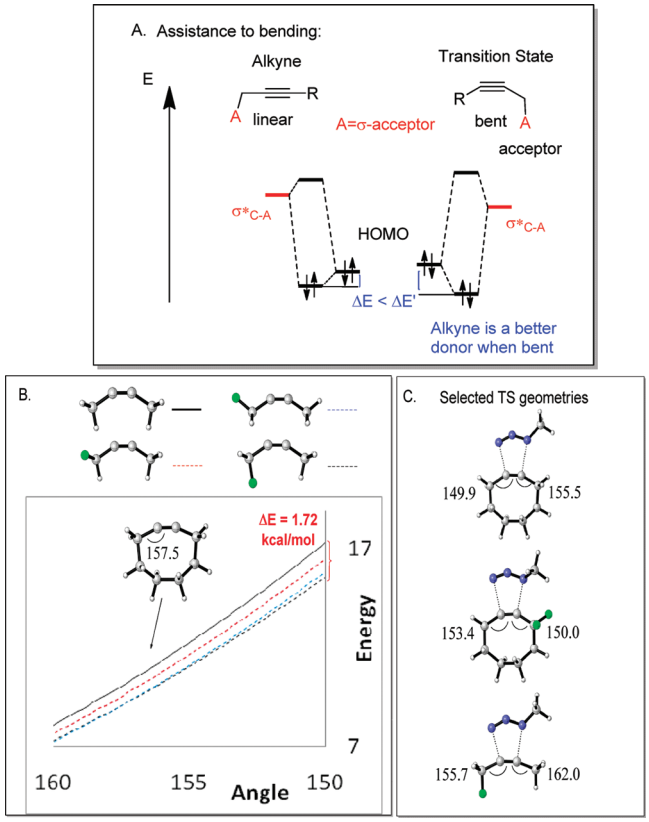

Figure 4. (A) FMO orbital changes upon alkyne bending responsible for the effect of acceptor substituents on the bending energy. (B) Relaxed energy scans (kcal/mol) for the symmetric bending of 2-butyne and 1-fluoro-2-butyne at the B3LYP/6-31G(d,p) level of theory. Cyclooctyne geometry is shown as a reference point for the relevant range of geometries. See Supporting Information for the full range of bending angles. (C) Average alkyne bending angles for three representative transition states are included for comparison (OCT/MeN_3, DIFO/MeN_3, *app*-1-fluoro-2-butyne/MeN_3). Energies are given in kcal/mol, angles in degrees.

effect is evident in its stereoelectronic features. The effect is maximized when the σ^*_{C-F} acceptor is antiperiplanar (*app*) to the in-plane π-system (e.g., 1.72 kcal/mol at the 150° C−C≡C angle typical for the cycloaddition TS). For the *syn*-periplanar arrangement the effect decreases slightly (1.64 kcal/mol). For the *gauche* arrangement, the stabilizing effect is even smaller (0.85 kcal/mol).

These observations are interesting because the effect of alkyne bending on HOMO energies, a potential driving force for intermolecular interactions with electrophiles, is believed to be relatively small[36] in comparison to the well-known enhancement of electrophilicity associated with LUMO energy[37] lowering in bent alkynes, e.g., benzyne.[38] Nevertheless, it is clear that the effect of the acceptor (~2 kcal/mol) should be experimentally significant.

dx.doi.org/10.1021/jo201434w | J. Org. Chem. 2012, 77, 75−89

Stereoelectronic Effects on Relative "Click" Reactivity. In order to determine to what extent this effect operates in the azide/alkyne cycloadditions, we have compared cycloaddition activation energies for 2-butyne[39] and 1-fluoro-2-butyne using methyl azide as the parent 1,3-dipole.

Importantly, the accelerating effect of fluorines is not manifested equally for the four stereo- and regioisomeric transition states of the 1-fluoro-2-butyne cycloaddition with methyl azide (Figure 5). In particular, the activation barriers are lowered

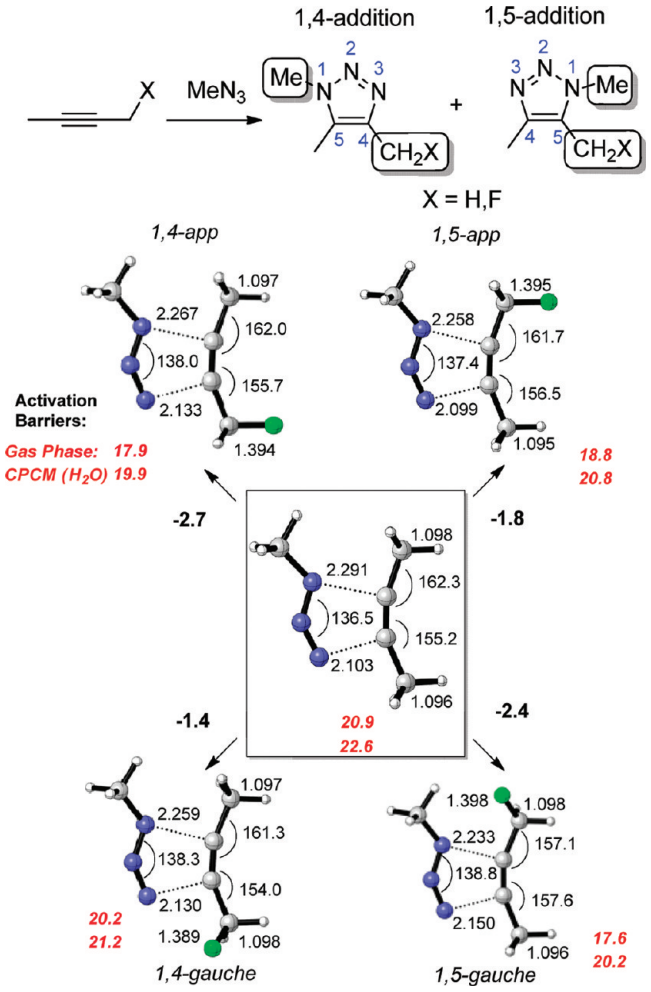

Figure 5. Geometries of the four transition states for the 1-fluoro-2-butyne/methyl azide cycloaddition calculated at the B3LYP/6-31G(d) level of theory (bottom) and numbering of atoms in the TS (top). Changes in the activation barriers due to fluorine introduction are shown in bold below the arrows. All energies are given in kcal/mol, bond lengths in Å, angles in degrees.

relative to the 2-butyne barrier when the σ^*_{C-F} orbital is antiperiplanar to the forming C−N bonds by 2.1 and 3.0 kcal/mol (for the 1,5- and 1,4-isomers, respectively).

A greater acceleration observed for the 1,4-isomer formation results from the asynchronous nature of the TS. The incipient N3···C4 distances are >0.1 Å shorter than the N1···C5 distances indicating that the N3−C4 bond formation is more pronounced at this stage. This is fully consistent with the ~5−7° greater bending at the C4 alkyne carbon observed in most cases (the unusual features of the 1,5-gauche TS will be discussed later). Greater bending and greater deviations from linearity observed at C4 suggest that this is the best place for attaching a hyperconjugative σ-acceptor.

In contrast, the activation barrier for 1,4-cycloaddition of the *gauche* conformer, where the C−F bond is misaligned with the in-plane alkyne π-system, is lowered by only 0.65 kcal/mol relative to the 2-butyne cycloaddition TS. In this context, the very low calculated barrier for the 1.5-*gauche* case (3.3 kcal/mol lowering relative to 2-butyne) looks surprising because this TS cannot also benefit from the aforementioned hyperconjugative assistance. This is not an isolated observation because the analogously low 1,5-*gauche* TS energy has been reported earlier by Houk and co-workers for the DIFO cycloaddition in the gas phase.[34] This effect can be traced to a stabilizing Me···F interaction that can be considered as a weak C−H···X hydrogen bond with a substantial electrostatic component. Because electrostatic stabilization is strongly attenuated once solvation effects are included in the calculation, the "hyperconjugation-assisted" 1,4-*app* cycloaddition becomes the lowest calculated energy reaction path in water and acetonitrile (2.7 kcal/mol barrier decrease and ~100-fold acceleration relative to 2-butyne). Since solvation effects are important, we will generally use the solvation-corrected data in our subsequent discussions.

Notably, the TS stabilization provided by a single fluorine substituent in the acyclic 1,4-antiperiplanar TS is greater than the TS stabilization provided by two fluorines in DIFO. This computational observation is consistent with the stereoelectronic nature of hyperconjugation and illustrates that the cyclooctyne frame imposes unfavorable restrictions on reaching the optimal orbital overlap with the C−F hyperconjugative acceptors in the TS.

Distortion Analysis. In order to understand the origin of the above accelerating effects better, we have turned to distortion analysis. Houk and co-workers have used this concept successfully toward a variety of cycloadditions.[34] This analysis dissects the activation barrier for cycloadditions into distortion and interaction energies. Distortion describes the energy penalty for adopting the TS geometry by the reactants, whereas interaction energy reflects energy lowering due to covalent and noncovalent interaction between the reactants. The data of distortion analysis are summarized in Table 1.

The distortion analysis readily rationalizes the anomalously low energy of the 1,5-*gauche* transition state where the interaction energy is 0.9 kcal/mol (2.2 kcal/mol in the gas phase) higher than for the 2-butyne TS. These numbers are consistent with the selective TS stabilization by an H-bond type C−H···F interaction corresponding to a relatively short (2.4 Å) H···F contact. NBO analysis suggests that the covalent component of this interaction is relatively small (hyperconjugative $n_F \rightarrow \sigma^*_{C-H}$ energy is 0.3 kcal/mol,[40] the same order of magnitude as the difference in the interaction energies for 1,4 and 1,5-*gauche* TS in water). The large part of stabilization is due to the Coulombic attraction between the two centers bearing significant charges (*vide infra*, "Electrostatics and Its Cooperative and Anticooperative Effects on Hyperconjugative Assistance").

Distortion energies for the two cycloadditions where the C−F bond is antiperiplanar to the breaking in-plane alkyne π-bond are lower than for the analogous processes where the C−F bonds are either gauche to the breaking bond or the acceptor σ^*_{C-F} orbital is absent (2-butyne). The lower distortion energies reflect the fact that their values include not only the destabilizing effects of alkyne bending but other electronic effects associated with the change of molecular geometry as well. TS-stabilization due to the

dx.doi.org/10.1021/jo201434w | J. Org. Chem. 2012, 77, 75−89

Table 1. Activation, Reaction, Distortion, and Interaction Energies for 2-Butyne and 1-Fluoro-2-butyne Transition States at the B3LYP/6-31G(d) level of theory

	E_{Dist} (kcal/mol)					
	alkyne	azide	total	E_{Int}, (kcal/mol)	$\Delta E^{\ddagger}$ (kcal/mol)	ΔE_{Rxn} (kcal/mol)
2-butyne	10.12	19.78	29.90	−9.01	20.89	−67.8
CPCM (H_2O)[a,b]	10.11	20.14	30.26	−7.66	22.62	−70.4
1,5-*app* gas phase	9.25	19.41	28.66	−9.83	18.83	−69.8
CPCM (H_2O)[a,b]	9.50	19.75	29.25	−8.41	20.84	−71.2
1,5-*gauche* gas phase	10.23	18.52	28.75	−11.20	17.55	−69.8
CPCM (H_2O)[a,b]	10.10	18.57	28.67	−8.52	20.15	−71.2
1,4-*app* gas phase	8.74	18.43	27.17	−9.27	17.90	−70.8
CPCM (H_2O)[a,b]	8.93	18.75	27.68	−7.77	19.91	−72.3
1,4-*gauche* Gas phase	10.16	18.52	28.68	−8.44	20.24	−70.8
CPCM (H_2O)[a,b]	10.06	18.85	28.91	−7.71	21.20	−72.3

[a]B3LYP/6-31G(d) geometry. [b]Radii = UA0.

hyperconjugative assistance is one of these effects (Figure 4), which is displayed via the apparent lowering of the alkyne distortion energy. The greater stabilization for the 1,4-*app* TS is consistent with the greater bending at C4.

An additional manifestation of selective TS stabilization is the increase of stabilizing interaction energy between the fragments. This difference fully accounts for the considerable deviations in the correlation of distortion energy with full activation barriers in Figure 6, shown to be reliable for this class of reactions on many occasions.[34]

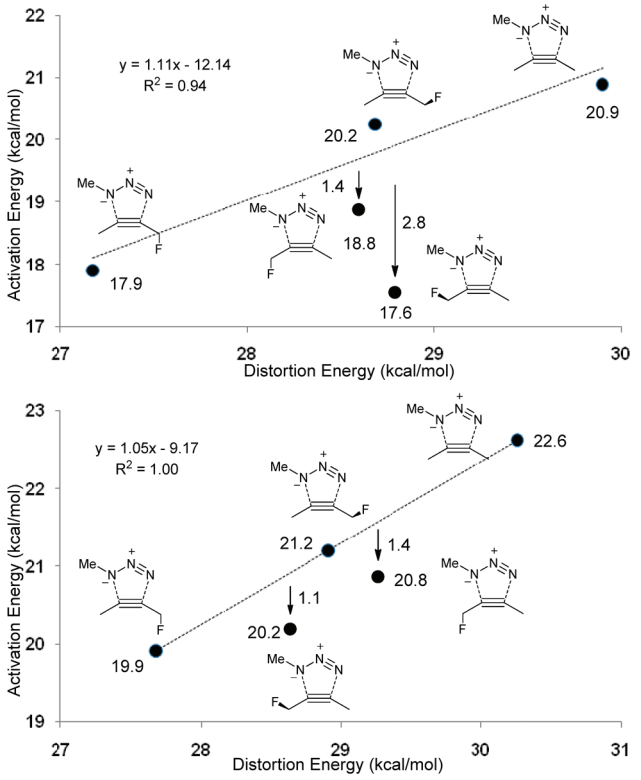

Figure 6. Correlation of the full distortion energy and activation energy for 2-butyne and 1-fluoro-2-butyne cycloadditions with methyl azide (B3LYP/6-31G*). (Top) Gas phase data. (Bottom) Single point solvation (water) correction. The energies below the straight line deviate from the distortion plot as a result of selective TS stabilization. (Gas phase: R^2 = 0.48, if all five points are included. CPCM (water): R^2 = 0.85, if all five points are included.)

Understanding the trends in interaction energy is, however, complicated because the overall interaction energy is comprised of covalent, steric and electrostatic components. Let us look at the stabilizing components of the interaction energy more carefully, hyperconjugation first, electrostatics next.

Natural Bond Orbital Dissection of Hyperconjugative Effects. NBO analysis can quantify stereoelectronic interactions in these systems. Even in the TS, the dominant NBO Lewis structure corresponds to the separated dipole and alkyne moieties, which makes comparison of hyperconjugative interactions with the linear and bent alkynes possible.

The results are revealing. Although distortion (bending) of the alkyne to the TS geometry does provide an increase in the $\pi \rightarrow \sigma^*_{C-F}$ interaction (on the order of 1 kcal/mol , consistent with the decrease in distortion energy and lowered bending energies in Figure 6), the most dramatic enhancement of hyperconjugative assistance by the σ^*_{C-F} orbitals is observed in the full TS where the azide is brought in direct proximity to the bent alkyne (Table 2). In this situation, the effect of hyperconjugation is estimated to be significantly larger! Stereoelectronic properties of these effects are illustrated by their dramatic enhancement for the antiperiplanar arrangement between the donor π_{in}-system and acceptor σ^*_{C-F} orbitals.

Table 2. NBO Analysis of Hyperconjugative Interactions Involved in the Methyl Azide Cycloaddition with 2-Butyne and 1-Fluoro-2-butyne (FB)[a]

	$\pi + \pi^* \rightarrow \sigma^*$ energies (kcal/mol)		
	linear alkyne	bent alkyne (TS geometry)	full transition state
2-butyne	3.27	2.99	3.75
1,4-*gauche* FB	8.96	8.86	8.84
1,4-*app* FB	8.96	9.99	14.43
1,5-*gauche* FB	8.96	9.39	10.40
1,5-*app* FB	8.96	9.56	15.54

[a]Only donation from the in-plane π-system (both π and π^*) is shown.

When viewed through the prism of the distortion analysis, this additional mechanism for TS stabilization should manifest itself in a different way, as an increase in "interaction energy" rather than a decrease in the "distortion energy". Increase in this interaction relative to the isolated alkyne is mostly due to an increase in the population of donor π^* orbital, which is empty in the reactant but gains 0.2 electrons in the TS (Table 3).

dx.doi.org/10.1021/jo201434w | J. Org. Chem. 2012, 77, 75−89

Table 3. NBO Analysis of In-Plane π/π^* Energy and Population Involved in the Methyl Azide Cycloaddition with 2-Butyne and the Four Conformers of 1-Fluoro-2-butyne[a]

	linear alkyne				bent alkyne (TS geometry)				full transition state			
	π_{in}		π^*_{in}		π_{in}		π^*_{in}		π_{in}		π^*_{in}	
	energy	pop	energy	pop	energy	pop	energy	pop	energy	pop	energy	pop
2-butyne	−6.95	1.965	4.27	0.055	−6.85	1.964	3.61	0.055	−6.95	1.727	3.37	0.193
1,4-*gauche*	−7.40	1.945	3.80	0.046	−7.35	1.966	3.15	0.057	−7.28	1.750	2.98	0.210
1,4-*app*	−7.40	1.945	3.80	0.046	−7.28	1.941	3.13	0.050	−7.23	1.731	3.06	0.196
1,5-*gauche*	−7.40	1.945	3.80	0.046	−7.37	1.966	3.15	0.057	−7.25	1.753	3.00	0.216
1,5-*app*	−7.40	1.945	3.80	0.046	−7.28	1.942	3.14	0.048	−7.27	1.719	3.07	0.203

[a]Energies are given in eV, orbital population in electrons.

Because the above interaction is manifested to a greater degree in the TS, this effect fits the classic definition of transition state stabilization, the ideal scenario for selective reaction acceleration.

Such relatively high population of a formally antibonding orbital in the NBO analysis is not surprising, considering the delocalized nature of transition states. It is typical for strongly delocalized systems (e.g., benzene, 1,3-butadiene, HF_2^-) where a single Lewis structure is insufficient. Figure 7 (top) illustrates

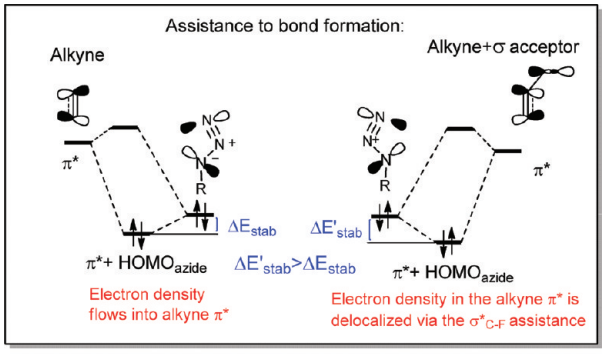

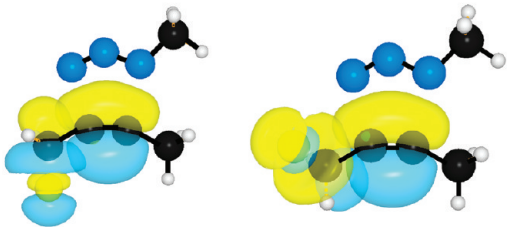

Figure 7. (Top) Electronic basis for TS stabilization. The increase in the alkyne π^* population due to the C···N bond-forming interaction complements the effect of propargylic acceptor on alkyne bending (Figure 3). (Bottom) NBO plots for orbital interactions between the propargylic σ-acceptors and the reacting in-plane alkyne π-bond in the cycloadditions TS for the optimal antiperiplanar (left) and suboptimal gauche (right) orbital arrangements.

orbital mixing for the highest in-plane occupied MO of the azide and $\pi^*_{in\text{-}plane}$ of the alkyne, which transfers electron density from the azide to the alkyne. Negative hyperconjugation with the stereoelectronically aligned σ^*_{C-F} orbital enhances this stabilizing interaction, which accounts for the second component of selective TS stabilization described above. Another way to understand the origin of the high π^*-population is provided by the curve crossing model of chemical reactivity where a transition state is described as an avoided crossing between ground and excited state configurations.[41]

Electrostatics and Its Cooperative and Anticooperative Effects on Hyperconjugative Assistance. Electrostatic effects on click reactivity were analyzed in two ways: (a) NBO charges in the full TS and in the isolated alkyne distorted to the TS geometry and (b) full ESP potentials of the four TS (Figure 8).

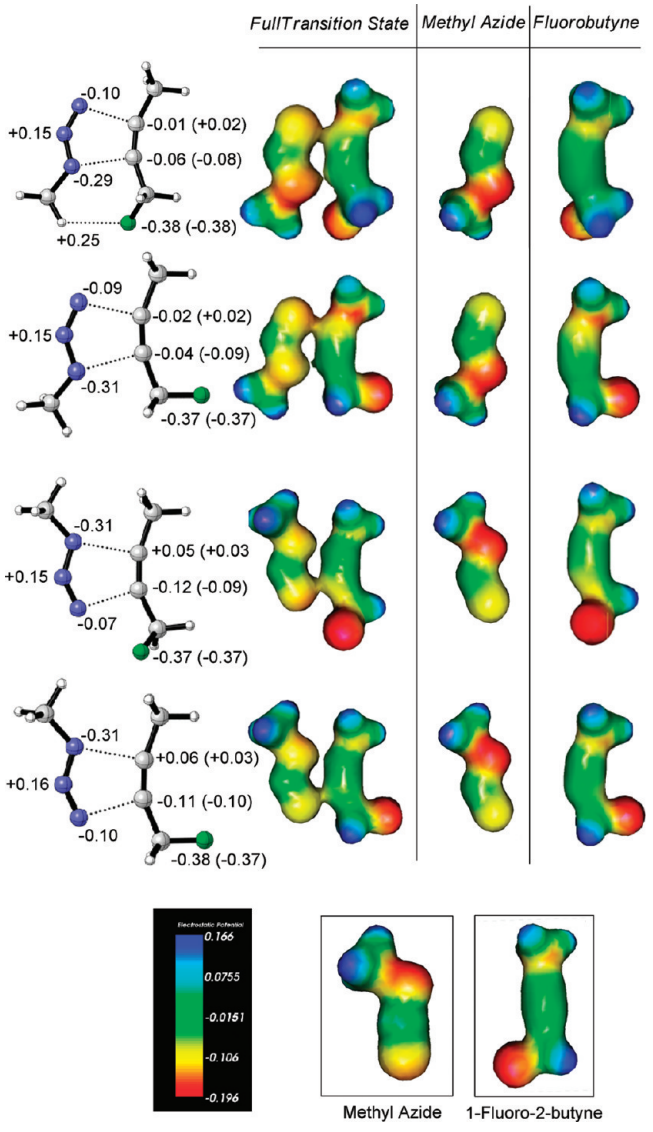

Figure 8. (Left) NBO atomic charges at the B3LYP/6-31G(d) level of theory (data in parentheses correspond to charges in the isolated alkyne distorted to the TS geometry). (Right) Electrostatic potential (ESP) surfaces. The ESP color coding and ESP surfaces for the alkyne and azide reagents in their unperturbed geometries are shown below.

dx.doi.org/10.1021/jo201434w | J. Org. Chem. 2012, 77, 75−89

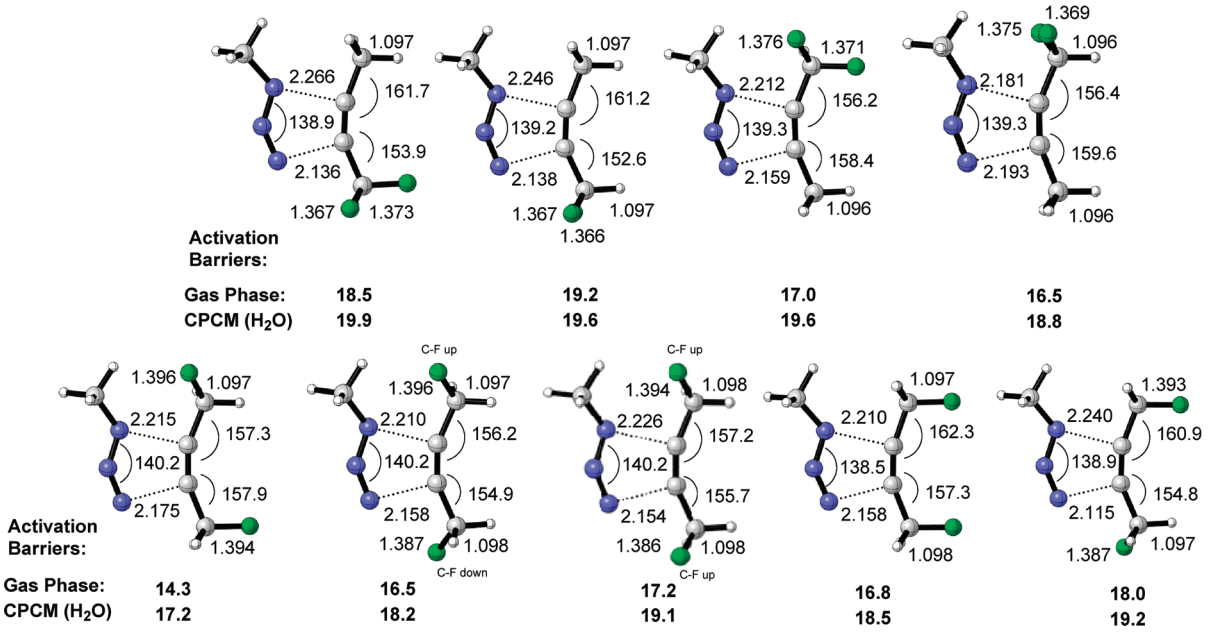

Figure 9. Geometries of the transition states of the 1,1-difluoro-2-butyne (top) and 1,4-difluoro-2-butyne (bottom)/methyl azide cycloaddition calculated at the B3LYP/6-31G(d) level of theory. All energies are given in kcal/mol, bond lengths in Å, angles in degrees.

Several observations are noteworthy. In particular, the N1 nitrogen of the azide bears significantly greater negative charge in comparison to the N3 nitrogen. This azide polarization creates unfavorable electrostatic interactions when the negative part of the alkyne dipole is oriented toward N3 (i.e., the 1,5-regiochemistry in the case of 1-fluoro-2-butyne). This observation suggests that more reactive azides can be designed via manipulation of charge distribution in the azide moiety.

The alkyne is polarized toward the CH_2F moiety. Interestingly, the alkyne polarization decreases upon the approach of azide along the 1,5-path but increases when azide approaches along the 1,4-trajectory. This difference is due to the more pronounced negative charge accumulation at the C2 carbon for 1,4-additions than for respective 1,5-additions (*gauche* vs *gauche* and *app* vs *app*) and due to additional changes in alkyne polarization, occurring as the azide approaches the bent alkyne. For 1,4-additions, the alkyne carbon α-to the CFH_2 group becomes *more* negatively charged in the presence of the azide, whereas for 1,5-additions, the same carbon becomes *less* negatively charged in the azide's proximity. Again, these contrasting changes in polarization are consistent with the greater antiperiplanar hyperconjugative assistance by the σ^*_{C-F} acceptor observed for the 1,4-regioselectivity.

Cooperativity of Hyperconjugative Effects: Click Reactivity of 1,4-Difluoro-2-butyne and 1,1-Difluoro-2-butyne. An intriguing conclusion from the above analysis is that propargylic fluorine atoms can accelerate both 1,4- and 1,5-addition via different mechanisms: hyperconjugative assistance for 1,4-addition and Me···F interaction for 1,5-addition. Since the two mechanisms are independent from each other, it is theoretically possible to combine them in a synergestic manner for achieving an even larger reaction acceleration.

Indeed, the calculated 1,4-difluorobutyne cycloaddition barrier where the TS combines the two accelerating effects is 5.4 kcal/mol (6.6 kcal/mol in the gas phase) lower in energy than the 2-butyne TS. The 2.7 and 3.0 kcal stabilization relative to the 1,4-*app* and 1,5-*gauche* TS for 1-fluorobutyne reveals remarkable additivity of the two effects (5.4 vs 3.0 + 2.7 kcal/mol).

In contrast, two fluorine atoms placed at the same propargylic carbon of 1,1-difluorobutyne cannot engage in hyperconjugative assistance and Me···F interaction at the same time, and a lower increase in reactivity is observed in comparison to that of the monofluorinated substrates. The lowest energy TS for this alkyne results from two Me···F interactions in the 1,5-cycloaddition geometry. The combined 3.8 kcal/mol stabilization from the two interactions indicates partial saturation of this effect: the second Me···F interaction is ~50% weaker (1.4 vs 2.4 kcal/mol, Figure 9).

Overall, the cooperativity effects are interesting and complex. Although their full discussion extends beyond the scope of this paper, we have summarized the effect of the second fluorine on the cycloaddition barriers in Figure 10.

Remarkably, the two 1,5-*gauche* interactions and one 1,4-*app* interaction in the 1,1,4-trifluoro-2-butyne cycloaddition TS shown in Figure 11 are sufficient to achieve the same acceleration as the full fluorination of both propargylic positions. The calculated gas phase cycloaddition barriers for both cases are essentially identical: ~12.5 kcal/mol. *The 8.4 kcal/mol barrier decrease in comparison to that of the 2-butyne cycloaddition, indicates that ~1 million-fold acceleration may be possible!* Solvation effects suggest that although this accelerating effect will be larger in nonpolar solvents than in water, such acceleration should be substantial in polar environments as well.

The "economic" use of fluorine effects via strategically accurate positioning of the C−F bonds is interesting from the practical perspective because the remaining positions at the propargylic carbons can be used for attaching other substituents (Figure 12). The combined effect of the three F-substituents eliminates *~80% of the barrier difference between 2-butyne and cyclooctyne without introducing any strain destabilization in the reactant*! Unfortunately, unlike the acyclic analogues, DIFO itself cannot benefit from the two effects identified in this paper at the same time because cyclic restraints render the optimal antiperiplanar position of a C−F bond impossible. Instead, DIFO relies on two effects, but only one at a time: (a) C−H···F

dx.doi.org/10.1021/jo201434w | J. Org. Chem. 2012, 77, 75−89

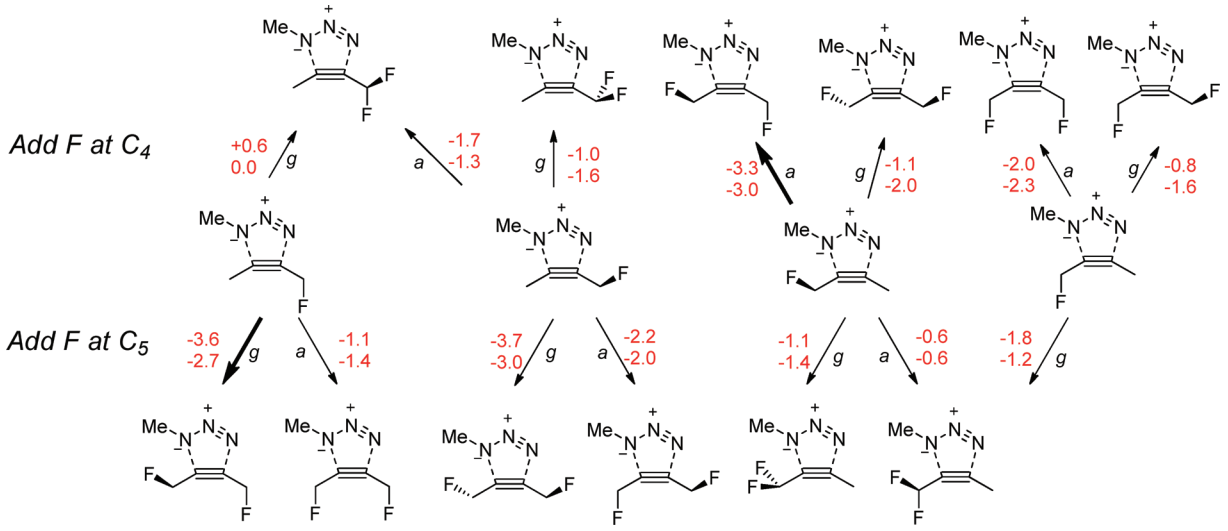

Figure 10. Contrasting effects of the second fluorine substituent on the cycloaddition barriers of difluorosubstituted 2-butynes with methyl azide at B3LYP/6-31G(d) level of theory. Activation energy changes are shown next to the arrows (top value: gas phase; bottom value: with solvation correction). The two interactions chosen for the further cooperative TS stabilization are shown with the bold arrows.

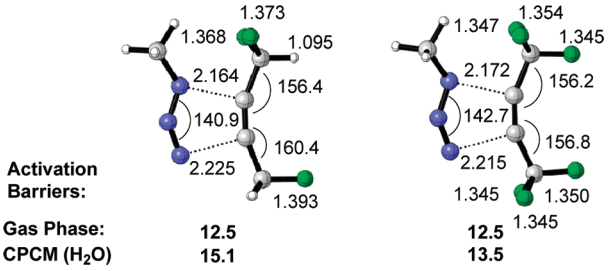

Figure 11. Geometries of the transition states of the 1,1,4-trifluoro-2-butyne (left) and perfluorobut-2-yne (right)/methyl azide cycloaddition calculated at the B3LYP/6-31G(d) level of theory. All energies are given in kcal/mol, bond lengths in Å, angles in degrees.

interactions in the 1,5-TS or (b) imperfect hyperconjugative assistance from the two gauche C−F bonds in the 1,4-TS. We will provide possible ways to overcome this limitation in our subsequent papers.

These accelerating effects should not be limited to fluorines. One can readily incorporate other H-bond acceptors near C_5 and other σ-acceptors near C_4 (Figure 12, bottom. See also the next section).

Competing Stabilizing Interactions: σ- versus π-Acceptors. In order to get further insights in the nature of TS stabilization in 1,3-dipolar cycloadditions, we have also compared relative acceleration provided by the σ^*_{C-F} acceptors with that of a typical carbonyl acceptor: $\pi^*_{C=O}$ of an ester. In the cycloadditions of 2-butynoates, several accelerating effects are possible, although not simultaneously. The Me···O interaction between the ester moiety and a propargylic C−H in the 1,5-TS has a close analogue in the Me···F electrostatic interaction mentioned above (1,5-*gauche*-TS). Similar to the trend observed in 1-fluoro-2-butyne, the Me···X interaction provides more stabilization in the gas phase, but when solvation corrections are taken into consideration, the conjugative interaction provides a greater TS stabilization. The delocalizing assistance by an ester can be manifested as conjugation or hyperconjugation (i.e, either as a $\pi \rightarrow \pi^*_{C-O}$ interaction between the breaking π bond of the alkyne and the π^* of the

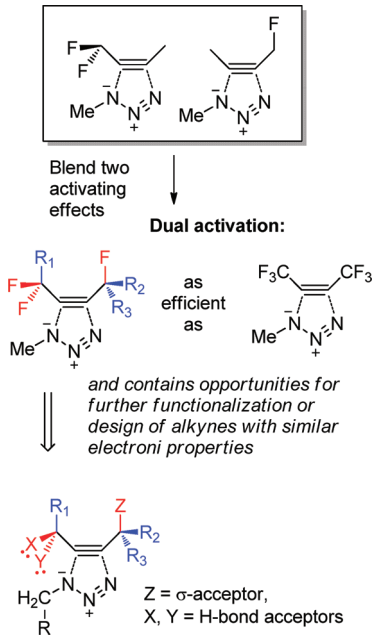

Figure 12. Favorable placement of fluorine substituents for optimal activation via cooperative effects and further possible variations in the design of reactive alkynes with suitable activation patterns.

carbonyl (Figure 13) or the analogous interaction with the carbonyl σ^*_{C-O}). The transition state geometries for the 1,4-isomer formation clearly indicate that the preferred assistance to the C−N bond formation is provided by the π^*_{C-O} orbital, in full agreement with the higher acceptor ability of π-bonds vs σ-bonds and the greater importance of conjugation[42] versus hyperconjugation. These preferences are consistent with the NBO energies for the stabilizing interactions in Figure 13.

Comparison of the two regioisomeric transition states reveals a more complex and interesting picture. The 90° rotation of the ester moiety in the transition state for the 1,5-isomer turns off the conjugative $\pi_{in} \rightarrow \pi^*_{C=O}$ stabilization and trades it for the combination of two effects outlined in the earlier section of this

dx.doi.org/10.1021/jo201434w | J. Org. Chem. 2012, 77, 75−89

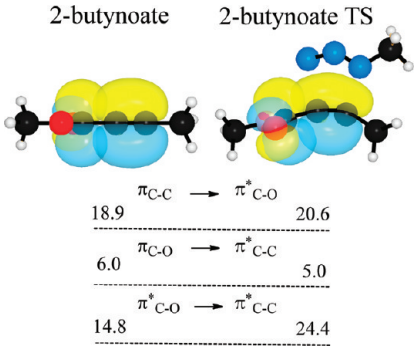

Figure 13. Changes in the magnitude of key alkyne/π-acceptor interactions leading to transition state stabilization in the methyl 2-butynoate/methyl azide cycloaddition. All NBO energies are in kcal/mol.

paper: the C−H···O interaction and the σ^*_{C-O} hyperconjugative assistance. The lower energy of the 1,5-TS indicates that together hyperconjugation plus C−H···O interaction can be more effective than the $\pi_{in} \rightarrow \pi^*_{C=O}$ conjugative assistance, especially in this system, where steric repulsion between the two groups further destabilizes the 1,4-TS.

In the fluorinated ester, the stabilizing effects can operate simultaneously. The electrostatic Me···X interaction can occur with either F or O, while the electronic assistance, either as the hyperconjugative $\pi \rightarrow \sigma^*_{C-F}$ interaction seen in fluorobutyne or as the conjugative $\pi \rightarrow \pi^*_{C-O}$ interaction, is possible in each regioisomer. In both the gas phase and in solution, the combination of Me···F interaction and $\pi \rightarrow \pi^*_{C-O}$ assistance provide the greatest stabilization (Figure 14).

Finally, we have also analyzed the effect of 2-pyridinyl substituent at the alkyne moiety. Similar to the ester group, this substituent can accelerate cycloadditions via three effects: hyperconjugative assistance (via σ^*_{C-N}), conjugative assistance (via aromatic π-system), and C−H···N interaction (via the lone pair of the pyridine nitrogen) following the general design outlined in Figure 12. Comparisons with the fluorinated ester are interesting: the ester → pyridine replacement at the fifth position increases the barrier by 1.4 kcal/mol, whereas the same change at the fourth position has a much larger effect (3.7 kcal/mol). As the result, the preferred position of the CF_3 group should change in the cycloadditions of the two alkynes.

Experimental Studies. A number of alkynes can be designed to manifest the synergy between the two effects discussed above as long as they contain a σ- or π-acceptor at one of the propargylic carbons and a heteroatom with a lone pair at the other propargylic position as outlined in Figure 12. In order to test the accuracy of computational methods and gain further insight into the nature and magnitude of the accelerating effects discussed in the previous section, we have determined the rates of cycloaddition for three systems outlined in the previous section. *p*-Fluorobenzyl azide was chosen as a model substrate for convenience, as the kinetics can be monitered via both ^{1}H and ^{19}F NMR spectroscopy. Comparison of calculated barriers suggested that reactivity of the three alkynes should follow the order methyl 4,4,4-trifluoro-2-butynoate > 2-(3,3,3-trifluoroprop-1-ynyl)pyridine > methyl 2-butynoate with the fluorinated ester being the most reactive (Figure 15).

The comparison of ethyl 2-butynoate **1** and ethyl 4,4,4-trifluoro-2-butynoate **2** allows us to get experimental information on the relative importance of two effects: (a) conjugation with a $\pi^*_{C=O}$ versus hyperconjugation with a

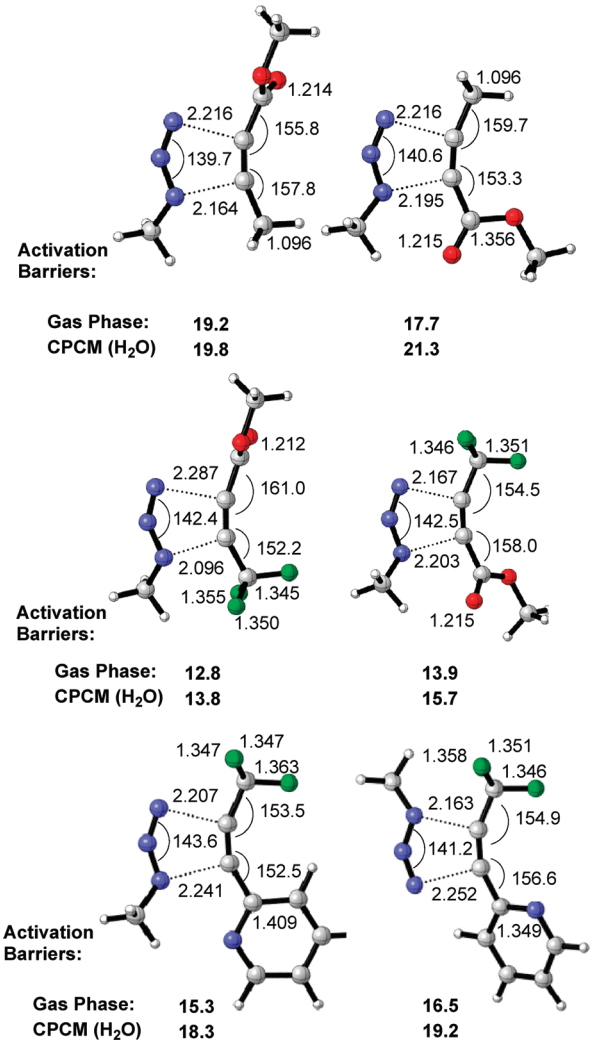

Figure 14. Geometries and energies of the cycloaddition transition states of methyl 2-butynoate (top), methyl 4,4,4-trifluoro-2-butynoate (middle), and (3,3,3-trifluoroprop-1-ynyl)pyridine (bottom) with methyl azide calculated at the B3LYP/6-31G* level of theory. All energies are given in kcal/mol, bond lengths in Å, angles in degrees.

σ^*_{C-F} and (b) and electronic differences between CF_3 and CH_3 discussed in the previous section. The pyridine moiety in alkyne **3** can provide either a σ^*_{C-N} hyperconjugative acceptor or nitrogen lone pair depending on the electronic demand in the cycloaddition TS. The CF_3-substituted substrates were prepared via vacuum pyrolysis of appropriately substituted phosphorus ylides (Figure 16).[43] Ethyl 2-butynoate is commercially available.

In each case, the cycloadditions proceeded smoothly to provide a mixture of two regioisomers. After chromatographic separation, the structures of the isomers were determined with 2D NMR techniques. In particular, the regiochemistry of cycloaddition is confirmed via the long-range HMBC correlations between benzylic hydrogens and the adjacent triazole carbon.

Although copper-free azide−alkyne cycloadditions of both ethyl 2-butynoate and ethyl 4,4,4-trifluoro-2-butynoate were reported earlier,[44] the kinetic comparison of their reactivity has not been conducted prior to this work. The differences in reactivity are dramatic (Figure 17). The cycloaddition of the fluorinated ester proceeds within hours at the room temperature and 0.5 M concentration of the reagents. The ~10^{-4} rate

dx.doi.org/10.1021/jo201434w | J. Org. Chem. 2012, 77, 75−89

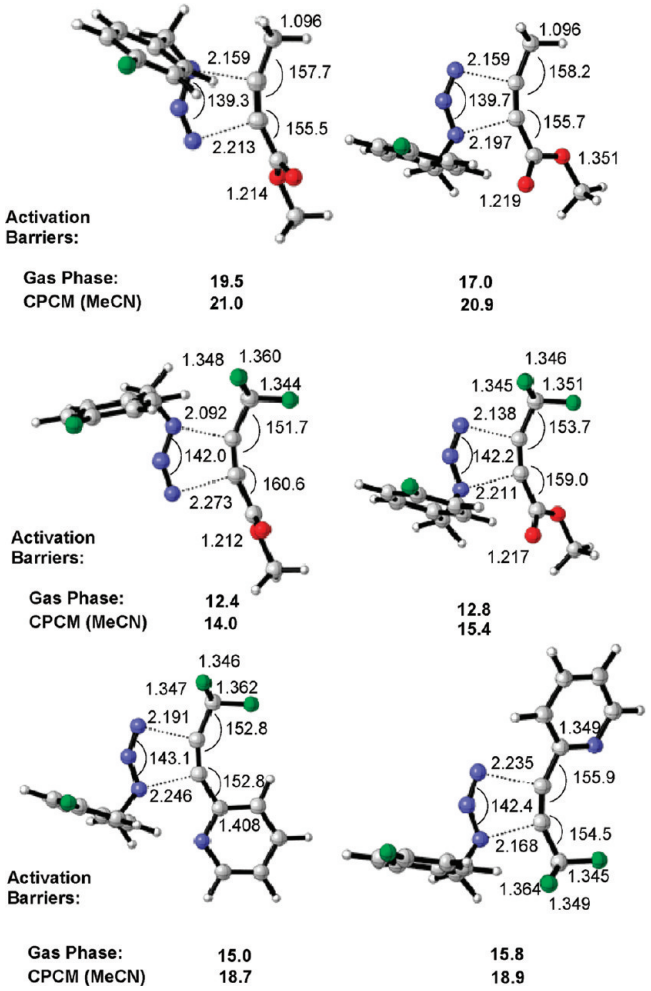

Figure 15. Geometries and energies of the transition states of methyl 2-butynoate (top), methyl 4,4,4-trifluoro-2-butynoate (middle), and 2-(3,3,3-trifluoroprop-1-ynyl)pyridine (bottom)/p-F-benzyl azide cycloadditions calculated at B3LYP/6-31G* levels of theory including zero point corrections. All energies are given in kcal/mol, bond lengths in Å, angles in degrees.

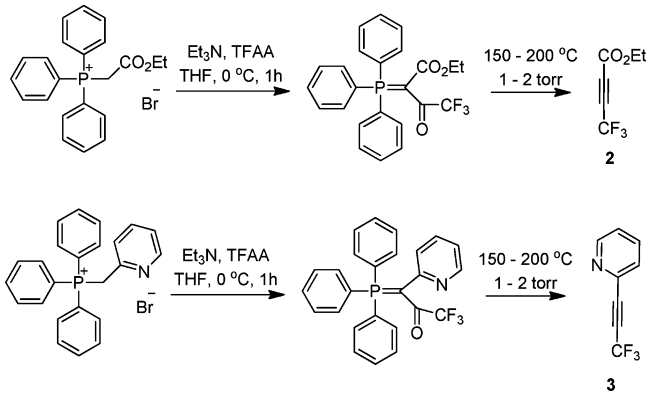

Figure 16. Synthesis of ethyl 4,4,4-trifluoro-2-butynoate **2** and 2-(3,3,3-trifluoroprop-1-ynyl)pyridine **3**.

constant at the biological temperature (~40 °C) is approaching that for the other alkynes used for bioconjugation.[17] In contrast, the reaction of ethyl 2-butynoate is very slow under these conditions and only occurs at a reasonable rate upon heating.[45] The rate constants for the formation of both regioisomers were determined for the three alkynes. Comparison of the rate constants for the two esters at 80 °C shows ~1000-fold acceleration of cycloaddition upon fluorination.

The relative rates for the formation of two regioisomers for each of the alkynes are particularly interesting. In full agreement with the stereoelectronic analysis presented in the previous sections, for the two alkynes **1** and **3** with a dominant acceptor substituent at the triple bond, the formation of the 1,4-isomer proceeds ~4−8 times faster. In contrast, the reaction of 4,4,4-trifluoro-2-butynoate, which bears *two* acceptor groups, provides the two isomers in an almost 1:1 ratio. Interestingly, in the latter case the formation of the 1,4-isomer, which positions the CF_3 group away from the benzyl substituent, becomes slightly favorable at the higher temperatures (see Supporting Information) suggesting that the formation of two regioisomers have different entropies of activation and, likely, the degree of organization in the TS.

The activation parameters for the formation of each of the two regioisomers were experimentally determined from the Arrhenius and Eyring plots (Figure 18). The activation enthalpy and entropy provided by the Eyring plots are especially useful in the case of ethyl 4,4,4-trifluoro-2-butynoate, where the regioisomer predicted to have a lower activation barrier, both in the gas phase and when single point corrections are considered, is major at room temperature and 40 °C but becomes minor at higher temperatures. The Eyring plot reveals this is due to entropic effects. The favorable interactions leading to transition state stabilization also lock in specific conformations, making these structures entropically less favorable. For both CF_3-substituted substrates, the proximity of alkyne trifluoromethyl to the azide methylene in the TS leads to a more negative activation entropy as the result of additional conformational rigidity in the TS, providing experimental evidence in favor of the C−H···F interactions identified in this work. In the cases of ethyl 2-butynoate and 2-(3,3,3-trifluoroprop-1-ynyl)pyridine, the regioisomer with the lower activation enthalpy also has a less negative entropy term, so the switch in selectivity is not observed.

The experimental activation energies for the formation of 1-(4-fluorobenzyl)-5-(trifluoromethyl)-1*H*-1,2,3,-triazole-4-carboxylate regioisomers are close to the computational data. The gas phase B3LYP data are in excellent agreement (within 0.1 kcal/mol) with the experimental values. The single point solvation correction brings the calculated barriers slightly higher than the experimental values, but still in reasonable agreement with the experiment. Although such close agreement is probably fortuitous because B3LYP is not expected to treat noncovalent interactions accurately, both theory and experiments agree that the lower energy TS is stabilized by both the Me···F electrostatic interaction and the $\pi \rightarrow \pi^*_{C-O}$ assistance. The experimental activation energies for the formation of 2-(3,3,3-trifluoroprop-1-ynyl)pyridine (middle) and ethyl 2-butynoate regioisomers also match reasonably well. Importantly, in both cases theory and experiments find the same regioisomer to be favored. The agreement between theory and experiment validates both the CH···X interactions and (hyper)conjugative assistance as sources of transition state stabilization in cycloaddition reactions, providing a benchmark for this level of theory and thus confirming its effectiveness in predicting relative trends useful for the future design of new reagents for copper-free click chemistry.

In summary, we have identified two stereoelectronic strategies for selective TS stabilization in catalyst-free azide/alkyne

dx.doi.org/10.1021/jo201434w | *J. Org. Chem.* 2012, 77, 75−89

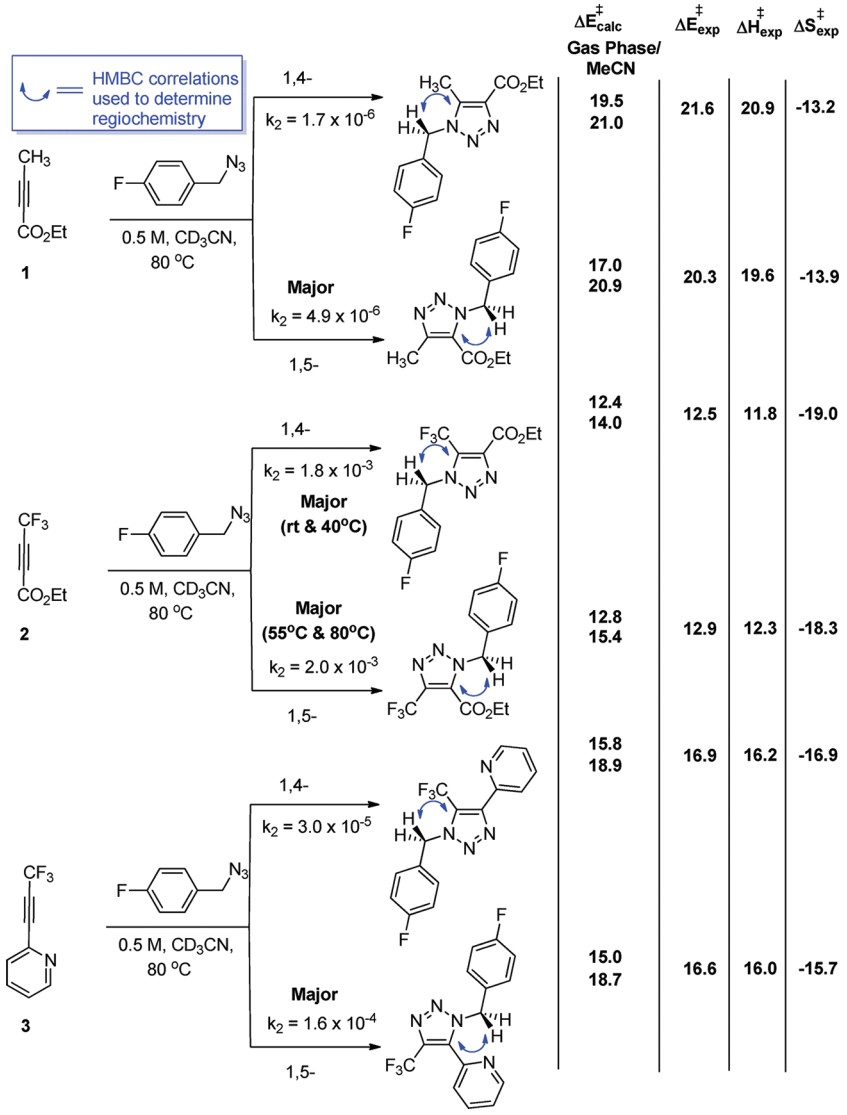

Figure 17. (Left) Rate constants (80 °C) for the formation of two regioisomers in the cycloaddition of activated alkynes **1**–**3** and long-range correlations in HMBC spectra used for the structural assignments. Full details are given in Supporting Information. (Right) $\Delta E^{\ddagger}_{calc}$, $\Delta E^{\ddagger}_{exp}$, $\Delta H^{\ddagger}_{exp}$, and $\Delta S^{\ddagger}_{exp}$, for each of the regioisomers in the cycloaddition of activated alkynes **1**–**3**. $\Delta E^{\ddagger}$ and $\Delta H^{\ddagger}$ are shown in kcal/mol, $\Delta S^{\ddagger}$ is given in cal/mol.

cycloadditions. Whereas the transition state for the formation of the 1,5-isomer can be stabilized via C–H···X interactions, both the 1,4- and 1,5-TS can be stabilized via hyperconjugative assistance for alkyne bending and for C···N bond formation. Such assistance provides a new strategy for efficient control of alkyne reactivity in click cycloadditions. DFT barriers suggest that judicious combination of the two independent TS-stabilizing effects can lead to ∼1 million-fold acceleration of cycloaddition with methyl azide. Experimental kinetic studies confirm large accelerating effects of σ-acceptors. Combination of the above strategies with strain activation and other noncovalent effects should lead to the rational design of robust acyclic and cyclic alkyne reagents for fast and tunable "click chemistry". Hyperconjugative assistance is not limited to alkynes but should be applicable to other π-systems as well. For example, the faster cycloaddition reactions of oxanorbornenes in comparison to their all-carbon analogues[46] can be attributed to the analogous TS stabilization imposed by the allylic σ^{*}_{C-O} orbitals.

EXPERIMENTAL SECTION

General Information. ^{1}H NMR and ^{13}C NMR spectra were recorded on a at 400 and 100 MHz correspondingly and at 600 and 150 MHz; ^{19}F NMR was recoreded at 375 MHz; and the 2D NMR experiments (HSQC and HMBC) were performed on a 600 MHz spectrometer. The chemical shifts are reported in parts per million (ppm) relative to the residual chloroform peak (7.26 ppm for ^{1}H NMR and 77.0 for ^{13}C NMR). Coupling constants are reported in hertz (Hz). IR spectra were recorded on a FTIR spectrometer with diamond ATR accessory as thin film. Mass spectra were recorded on a MS JMS 600H spectrometer. GS–MS analyses were performed on GS system with DB-5MS+DG 30 m × 0.25 mm, 0.25 μm capillary column coupled with MS detector.

Yields refer to isolated material judged to be >95% pure by ^{1}H NMR spectroscopy following silica gel chromatography (F-254 silica, 230–499 mesh particle size). All chemicals were used as received unless otherwise noted.

4-Fluorobenzyl Azide.

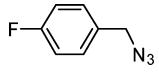

dx.doi.org/10.1021/jo201434w | J. Org. Chem. 2012, 77, 75–89

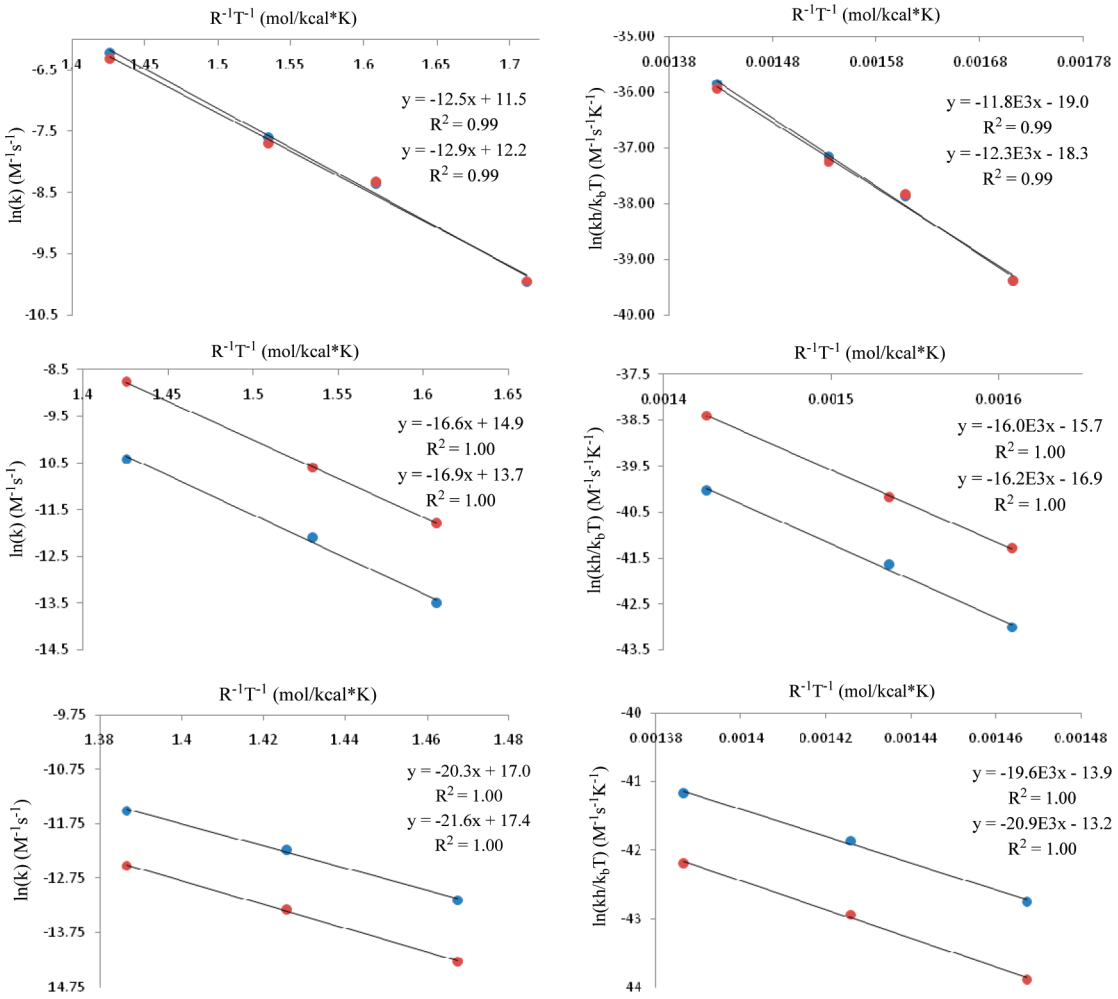

Figure 18. Arrhenius (left) and Eyring (right) plots for cycloaddition of ethyl 4,4,4-trifluoro-2-butynoate (top), 2-(3,3,3-trifluoroprop-1-ynyl)pyridine (middle), and ethyl 2-butynoate (bottom) with *p*-fluorobenzyl azide.

A mixture of 4-fluorobenzyl bromide (1.7 g, 8.91 mmol) and sodium azide (1.45 g, 22.27 mmol) in 17 mL of DMF was stirred under a nitrogen atmosphere for 4 h at 60 °C. The reaction mixture was cooled, quenched with 150 mL of water, and extracted with benzene (since diethyl ether was unavailable). The organic layer was washed with brine and dried with Na_2SO_4, and the solvent was removed under reduced pressure to afford 1.4 g of crude *p*-fluorobenzyl azide. Purification by column chromatography afforded 0.90 g (67%) of the pure product. Spectral data were in good agreement with the literature.[47] ^{1}H NMR ($CDCl_3$, 400 MHz): δ 4.31 (s, 2H), 7.05−7.10 (m, 2H), 7.28−7.31 (m, 2H).

Ethyl 4,4,4-Trifluoro-3-oxo-2-(triphenylphosphoranylidene) Butanoate.

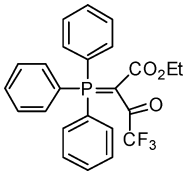

Acylation of the (carbethoxymethyl)triphenylphosphonium bromide with trifluoroacetic anhydride in the presence of triethylamine was carried out following a literature procedure.[43] Spectral data for the product was in good agreement with literature.Yield 11 g (89%); ^{1}H NMR ($CDCl_3$, 400 MHz): δ 0.86 (t, 3H), 3.80 (q, 2H), 7.48−7.51 (m, 6H), 7.57 (m, 3H), 7.65 (m, 6H)

1,1,1-Trifluoro-3-pyridin-2-yl-3-(triphenylphosphoranylidene) Acetone.

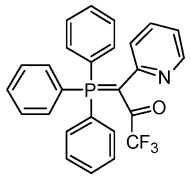

Acylation of the (triphenyl(pyridin-2-ylmethyl)phosphonium chloride with trifluoroacetic anhydride in the presence of triethylamine was carried out analogous to a literature procedure,[43] affording 1,1,1-trifluoro-3-pyridin-2-yl-3-(triphenylphosphoranylidene)acetone. Yield 4.5 g (91%), white crystals, mp 97−99 °C. ^{1}H NMR (400 MHz, $CDCl_3$): δ 6.85 (t, J = 6.0 Hz, 1H), 7.28 (d, J = 7.8 Hz, 1H), 7.37−7.42 (m, 7H), 7.49−7.53 (m, 3H), 7.59−7.64 (m, 6H), 6.19 (d, J = 4.0 Hz, 1H). ^{13}C NMR (150 MHz, $CDCl_3$): δ 0.0, 120.6, 123.9, 124.8, 128.7, 128.8, 129.5, 132.2, 132.2, 133.7, 133.8, 135.4, 148.7. ^{19}F NMR (377 MHz, $CDCl_3$): δ −68.7. HRMS (EI): calcd for $C_{26}H_{19}F_3NOP$ 449.1151, found 449.1149.

dx.doi.org/10.1021/jo201434w | *J. Org. Chem.* 2012, 77, 75−89

Ethyl 4,4,4-Trifluoro-2-butynoate.

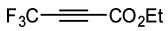

Thermolysis of 4,4,4-trifluoro-3-oxo-2-(triphenylphosphoranylidene)butanoate at 190−230 °C (ca. 1 mmHg) according to the known procedure gave ethyl 4,4,4-trifluoro-2-butynoate.[43] Spectral data was in good agreement with previous literature reports. Yield 2.9 g (79%). ^{1}H NMR ($CDCl_3$, 400 MHz): δ 1.38 (t, 3 H, J = 7.16), 4.40 (q, 2 H, J = 7.16)

2-(3,3,3-Trifluoroprop-1-ynyl)pyridine.[48]

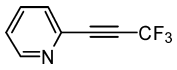

Thermolysis of 1,1,1-trifluoro-3-pyridin-2-yl-3-(triphenylphosphoranylidene)acetone gave 2-(3,3,3-trifluoroprop-1-ynyl)pyridine. Yield 0.98 g (57%), colorless liquid, bp 153−155 °C. ^{1}H NMR (400 MHz, CD_3CN): δ 7.40 (ddd, J = 7.5, 4.9, 0.8 Hz, 1H), 7.60 (d, J = 7.5 Hz, 1H), 7.76 (dt, J = 7.5, 1.9 Hz, 1H), 8.67 (d, J = 4.9 Hz, 1H). ^{19}F NMR (377 MHz, CD_3CN): δ −51.1.

Cycloadditions. Ethyl 4,4,4-Trifluoro-2-butynoate. Reaction of 0.17 g (1 mmol) of ethyl 4,4,4-trifluoro-2-butynoate and 0.15 g (1 mmol) of *p*-fluorobenzyl azide in CH_3CN at 22 °C provided two products as a mixture of stereoisomers, which were separated by column chromatography.

Ethyl 1-(4-Fluorobenzyl)-4-(trifluoromethyl)-1*H*-1,2,3-triazole-5-carboxylate.

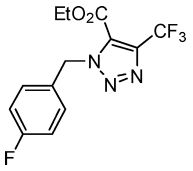

Yield 0.147 g (46%), colorless oil. ^{1}H NMR (600 MHz, $CDCl_3$): δ 1.37 (t, J = 7.2 Hz, 3H), 4.40 (q, J = 7.2 Hz, 2H), 5.90 (s, 2H), 7.40 (t, J = 8.7 Hz), 7.38 (dd, J = 8.7, 5.3 Hz). ^{13}C NMR (150 MHz, $CDCl_3$): δ 13.6 (CH_3), 53.4 ($\underline{C}H_2$−Ph), 63.0 (OCH_2), 116.0 (d, J = 22.0 Hz, 2C), 119.8 (q, J = 268.5 Hz, CF_3), 126.5 ($C_{triazole}$), 129.8 (C_q), 130.4 (d, J = 8.8 Hz, 2C), 139.9 (q, J = 39.6 Hz, $\underline{C}$−CF_3), 156.9 (CO), 163.0 (d, J = 248.7 Hz, C_q). ^{19}F NMR (377 MHz, $CDCl_3$): δ −112.4, −60.9. HRMS (EI): calcd for $C_{13}H_{11}F_4N_3O_2$ 317.0787, found 317.0787.

Ethyl 1-(4-Fluorobenzyl)-5-(trifluoromethyl)-1*H*-1,2,3-triazole-4-carboxylate.

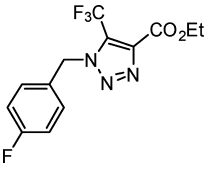

Yield 0.130 g (41%), colorless oil. ^{1}H NMR (600 MHz, $CDCl_3$): δ 1.41 (t, J = 7.3 Hz, 3H), 4.45 (q, J = 7.3 Hz, 2H), 5.74 (s, 2H), 7.06 (t, J = 8.5 Hz), 7.38 (dd, J = 8.5, 5.3 Hz). ^{13}C NMR (150 MHz, $CDCl_3$): δ 14.0 (CH_3), 54.3 ($\underline{C}H_2$−Ph), 62.3 (OCH_2), 116.1 (d, J = 22.0 Hz, 2C), 119.1 (q, J = 270.7 Hz, CF_3), 128.3 (q, J = 42.9 Hz, $\underline{C}$−CF_3), 129.1(C_q), 129.6 (d, J = 8.8 Hz, 2C), 139.8 ($C_{triazole}$), 158.9 (CO), 163.1 (d, J = 248.7 Hz, C_q). ^{19}F NMR (377 MHz, $CDCl_3$): δ −112.0, −56.5. HRMS (EI): calcd for $C_{13}H_{11}F_4N_3O_2$ 317.0787, found 317.0787.

Ethyl 2-Butynoate. Reaction of 0.11 g (1 mmol) of ethyl 2-butynoate and 0.15 g (1 mmol) of *p*-fluorobenzyl azide at 80 °C (neat) provided two products as a mixture of stereoisomers, which were separated by column chromatography.

Ethyl 1-(4-Fluorobenzyl)-4-methyl-1*H*-1,2,3-triazole-5-carboxylate.

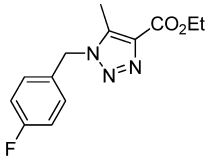

Yield 0.06 g (24%), colorless oil. ^{1}H NMR (600 MHz, $CDCl_3$): δ 1.37 (t, J = 7.3 Hz, 3H), 2.54 (s. 3H), 4.36 (q, J = 7.3 Hz, 2H), 5.85 (s, 2H), 7.01 (t, J = 8.8 Hz), 7.32 (dd, J = 8.8, 5.3 Hz). ^{13}C NMR (150 MHz, $CDCl_3$): δ 12.5 (CH_3−Ar), 14.1 ($\underline{C}H_3CH_2$), 53.1 ($\underline{C}H_2$−Ph), 61.5 (OCH_2), 115.5 (d, J = 20.9 Hz, 2C), 124.2 ($C_{triazole}$), 129.8 (d, J = 7.7 Hz, 2C), 131.2 (C_q), 148.6 ($C_{triazole}$), 156.9 (CO), 162.6 (d, J = 247.6 Hz, C_q). ^{19}F NMR (377 MHz, $CDCl_3$): δ −113.6. HRMS (EI): calcd for $C_{13}H_{14}FN_3O_2$ 263.1070, found 263.1070.

Ethyl 1-(4-Fluorobenzyl)-5-methyl-1*H*-1,2,3-triazole-4-carboxylate.

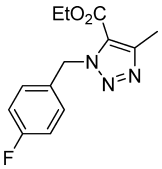

Yield 0.18 g (69%), colorless oil. ^{1}H NMR (600 MHz, $CDCl_3$): δ 1.42 (t, J = 7.3 Hz, 3H), 2.47 (s. 3H), 4.41 (q, J = 7.3 Hz, 2H), 5.52 (s, 2H), 7.04 (t, J = 8.7 Hz), 7.18 (dd, J = 8.7, 5.3 Hz). ^{13}C NMR (150 MHz, $CDCl_3$): δ 9.0, 14.3, 51.2, 60.9, 116.0 (d, J = 22.0 Hz), 129.0 (d, J = 8.8 Hz), 137.0, 138.1, 161.6, 162.7 (d, J = 248.7 Hz). ^{19}F NMR (377 MHz, $CDCl_3$): δ −112.8. HRMS (EI): calcd for $C_{13}H_{14}FN_3O_2$ 263.1070, found 263.1070.

2-(3,3,3-Trifluoroprop-1-ynyl)pyridine. Reaction of 0.17 g (1 mmol) of 2-(3,3,3-trifluoroprop-1-ynyl)pyridine and 0.15 g (1 mmol) of *p*-fluorobenzyl azide in CH_3CN (2 mL) at 80 °C provided two products as a mixture of stereoisomers, which were separated by column chromatography.

2-(1-(4-Fluorobenzyl)-5-(trifluoromethyl)-1*H*-1,2,3-triazol-4-yl)pyridine.

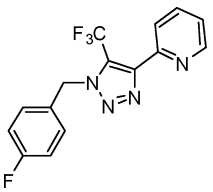

Yield 0.24 g (76%), colorless oil. ^{1}H NMR (600 MHz, $CDCl_3$): δ 5.81 (s, 2H), 6.89 (t. 2H, J = 8.52 Hz), 7.03 (t, 2H), 7.44 (m, 2H), 7.79 (t, 1H), 8.80 (d, 1H, J = 4.56 Hz). ^{13}C NMR (150 MHz, $CDCl_3$$\delta$ 9.0 (CH_3−Ar), 14.3 ($\underline{C}H_3CH_2$), 51.2 ($\underline{C}H_2$−Ph), 60.9 (OCH_2), 116.0 (d, J = 22.0 Hz, 2C), 129.0 (d, J = 8.8 Hz, 2C), 137.0 ($C_{triazole}$), 138.1 ($C_{triazole}$), 161.6 (CO), 162.7 (d, J = 248.7 Hz, C_q). ^{19}F NMR: δ −56.09, −112.59. HRMS (ESI+): calcd for $C_{15}H_{10}F_4N_4$ 345.0739, found 345.0751.

dx.doi.org/10.1021/jo201434w | J. Org. Chem. 2012, 77, 75−89

2-(1-(4-Fluorobenzyl)-4-(trifluoromethyl)-1*H*-1,2,3-triazol-5-yl)pyridine.

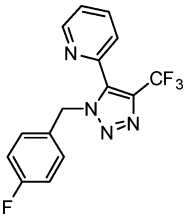

Yield 0.05 g (17%), colorless oil. ^{1}H NMR (600 MHz, $CDCl_3$): δ 5.74 (s, 2H), 7.06 (m, 2H), 7.30 (m, 3H), 7.81 (m, 1H), 7.93 (d, 1H, J = 7.92), 8.68 (d, 1H, J = 4.56). ^{13}C NMR (150 MHz, $CDCl_3$): δ 53.0, 114.9 (d, J = 21.9), 122.4 (d, J = 51.5), 128.6 (d, J = 8.52), 135.6, 147.2 (d, J = 76.2), 148.6, 161.1 (d, J = 246.4). ^{19}F NMR: δ −59.2, −113.03. HRMS (ESI+): calcd for $C_{15}H_{10}F_4N_4$ 345.0739, found 345.0736.

■ ASSOCIATED CONTENT

Supporting Information

Geometries, energies and distortion analysis for all reactants, products and transition states, 1D and 2D NMR spectra of synthetic intermediates and products. This material is available free of charge via the Internet at http://pubs.acs.org.

■ AUTHOR INFORMATION

Corresponding Author

*E-mail: alabugin@chem.fsu.edu.

■ ACKNOWLEDGMENTS

I.A. and G.D. are grateful to the National Science Foundation (Grants CHE-0848686 and CHE-0749918) for support of this research project.

■ REFERENCES

(1) (a) Kolb, H. C.; Finn, M. G.; Sharpless, K. B. *Angew. Chem., Int. Ed.* **2001**, *40*, 2004−2021. (b) Special Issue on Click Chemistry: Finn, M. G.; Fokin, V. V., Guest Eds. *Chem. Soc. Rev.* **2010**, *39*, 1221.

(2) Tron, G. C.; Pirali, T.; Billington, R. A.; Canonico, P. L.; Sorba, G.; Genazzani, A. A. *Med. Res. Rev.* **2008**, *28*, 278.

(3) (a) Jewett, J. C.; Bertozzi, C. R. *Chem. Soc. Rev.* **2010**, *39*, 1272. (b) Ning, X.; Guo, J.; Wolfert, M.; Boons, G.-J. *Angew. Chem., Int. Ed.* **2008**, *47*, 2253. (c) Sletten, E. M.; Bertozzi, C. R. *Acc. Chem. Res.* **2011**, *44*, 666.

(4) Binder, W. H.; Sachsenhofer, R. *Macromol. Rapid Commun.* **2007**, *28*, 15.

(5) Huang, S.; Clark, R. J.; Zhu, L. *Org. Lett.* **2007**, *9*, 4999. Hua, Y.; Flood, A. H. *Chem. Soc. Rev.* **2010**, *39*, 1262.

(6) Golas, P. L.; Tsarevsky, N. V.; Sumerlin, B. S.; Matyjaszewski, K. *Macromolecules* **2006**, *39*, 6451.

(7) Rostovtsev, V. V.; Green, L. G.; Fokin, V. V.; Sharpless, K. B. *Angew. Chem., Int. Ed.* **2002**, *41*, 2596.

(8) Tornoe, C. W.; Christensen, C.; Meldal, M. *J. Org. Chem.* **2002**, *67*, 3057.

(9) Huisgen, R. *1,3-Dipolar cycloaddition chemistry*; Padwa, A, Ed.; John Wiley &Sons: New York, 1987; Vol. *1*.

(10) (a) Hein, J. E.; Fokin, V. V. *Chem. Soc. Rev.* **2010**, *39*, 1302. (b) Tornøe, C. W.; Meldal, M. *Chem. Rev.* **2008**, *108*, 2952. (c) Moses, J. E.; Moorhouse, A. D. *Chem. Soc. Rev.* **2007**, *36*, 1249.

(11) The toxicity of Cu salts can be significantly alleviated by a suitable choice of Cu-coordinating ligands: Hong, V.; Steinmetz, N. F.; Manchester, M.; Finn, M. G. *Bioconjugate Chem.* **2010**, *21*, 1912.

(12) (a) Blomquist, A. T.; Liu, L. H. *J. Am. Chem. Soc.* **1953**, *75*, 2153. (b) Wittig, G.; Krebs, A. *Chem. Ber.* **1961**, *94*, 3260. (c) Wittig, G.; Pohlke., R. *Chem. Ber.* **1961**, *94*, 3276.

(13) Codelli, J. A.; Baskin, J. M.; Agard, N. J.; Bertozzi, C. R. *J. Am. Chem. Soc.* **2008**, *130*, 11486.

(14) (a) Ning, X.; Guo, J.; Wolfert, M. A.; Boons, G.-J. *Angew. Chem., Int. Ed.* **2008**, *47*, 2253. (b) Poloukhtine, A. A.; Mbua, N. E.; Wolfert, M. A.; Boons, G.-J.; Popik, V. V. *J. Am. Chem. Soc.* **2009**, *131*, 15769. (c) Sanders, B. C.; Friscourt, F.; Ledin, P. A.; Mbua, N. E.; Arumugam, S.; Guo, J.; Boltje, T. J.; Popik, V. V.; Boons, G.-J. *J. Am. Chem. Soc.* **2011**, *133*, 949.

(15) Becer, C. R.; Hoogenboom, R.; Schubert, U. S. *Angew. Chem., Int. Ed.* **2009**, *48*, 4900.

(16) Baskin, J. M.; Bertozzi, C. R. *Aldrichimica Acta* **2010**, *43*, 15.

(17) Reviews on bioorthogonal chemistry: (a) Sletten, E. M.; Bertozzi, C. R. *Angew. Chem., Int. Ed.* **2009**, *48*, 6974. (b) Lim, R. K. V.; Lin, Q. *Chem. Commun.* **2010**, *46*, 1589.

(18) (a) Agard, N. J.; Prescher, J. A.; Bertozzi, C. R. *J. Am. Chem. Soc.* **2004**, *126*, 15046; Addition/Correction: *J. Am. Chem. Soc.* **2005**, *127*, 11196. (b) Jewett, J. C.; Bertozzi, C. R. *Chem. Soc. Rev.* **2010**, *39*, 1272.

(19) Chang, P. V.; Prescher, J. A.; Sletten, E. M.; Baskin, J. M.; Miller, I. A.; Agard, N. J.; Lo, A.; Bertozzi, C. R. *Proc. Natl. Acad. Sci. U.S.A.* **2010**, *107*, 1821.

(20) Jewett, J. C.; Sletten, E. M.; Bertozzi, C. R. *J. Am. Chem. Soc.* **2010**, *132*, 3688.

(21) Some acceleration can be achieved via removal of steric interactions in the TS. For example, Goddard identified negative steric interactions between *o*-hydrogens of the benzene rings of DIBO and the alkyl azide. Chenoweth, K.; Chenoweth, D.; Goddard, W. A. III *Org. Biomol. Chem.* **2009**, *7*, 5255 . Tummatorn and Dudley reported SPAAC coupling of a benzocyclononyne that included a methylene spacer to minimize this steric interaction; see ref 25f.

(22) Ess, D. H.; Jones, G. O.; Houk, K. N. *Org. Lett.* **2008**, *10*, 1633.

(23) (a) Alabugin, I. V. *J. Org. Chem.* **2000**, *65*, 3910. (b) Alabugin, I. V.; Manoharan, M.; Kovalenko, S. V. *Org. Lett.* **2002**, *4*, 1119. (c) Alabugin, I. V.; Manoharan, M. *J. Phys. Chem. A* **2003**, *107*, 3363. (d) Alabugin, I. V.; Manoharan, M.; Zeidan, T. A. *J. Am. Chem. Soc.* **2003**, *125*, 14014. (e) Alabugin, I. V.; Manoharan, M. *J. Org. Chem.* **2004**, *69*, 9011. (f) Alabugin, I. V.; Manoharan, M. *J. Comput. Chem.* **2007**, *28*, 373. (g) Alabugin, I. V.; Gilmore, K.; Peterson, P. *WIREs Comput. Mol. Sci.* **2011**, *1*, 109.

(24) (a) Zeidan, T. A.; Kovalenko, S. V.; Manoharan, M.; Clark, R. J.; Ghiviriga, I.; Alabugin, I. V. *J. Am. Chem. Soc.* **2005**, *127*, 4270. (b) Alabugin, I. V.; Manoharan, M. *J. Am. Chem. Soc.* **2003**, *125*, 4495. (c) Breiner, B.; Schlatterer, J. C.; Kovalenko, S. V.; Greenbaum, N. L.; Alabugin, I. V. *Proc. Natl. Acad. Sci. U.S.A.* **2007**, *104*, 13016. (d) Breiner, B.; Schlatterer, J. C.; Kovalenko, S. V.; Greenbaum, N. L.; Alabugin, I. V. *Angew. Chem., Int. Ed.* **2006**, *45*, 3666. (e) Vasilevsky, S. F.; Mikhailovskaya, T. F.; Mamatyuk, V. I.; Bogdanchikov, G. A.; Manoharan, M.; Alabugin, I. V. *J. Org. Chem.* **2009**, *74*, 8106. (f) Alabugin, I. V.; Gilmore, K.; Patil, S.; Manoharan, M.; Kovalenko, S. V.; Clark, R. J.; Ghiviriga, I. *J. Am. Chem. Soc.* **2008**, *130*, 11535. (g) Yang, W.-Y.; Breiner, B.; Kovalenko, S. V.; Ben, C.; Singh, M.; LeGrand, S. N.; Sang, Q.-X.; Strouse, G. F.; Copland, J. A.; Alabugin, I. V. *J. Am. Chem. Soc.* **2009**, *131*, 11458. (h) Vasilevsky, S. F.; Baranov, D. S.; Mamatyuk, V. I.; Gatilov, Y. V.; Alabugin, I. V. *J. Org. Chem.* **2009**, *74*, 6143. (i) Alabugin, I. V.; Manoharan, M. *J. Am. Chem. Soc.* **2005**, *127*, 12583. (j) Alabugin, I. V.; Manoharan, M. *J. Am. Chem. Soc.* **2005**, *127*, 9534. (k) Zeidan, T.; Manoharan, M.; Alabugin, I. V. *J. Org. Chem.* **2006**, *71*, 954. (l) Baroudi, A.; Mauldin, J.; Alabugin, I. V. *J. Am. Chem. Soc.* **2010**, *132*, 967. (m) Alabugin, I. A.; Gilmore, K.; Manoharan, M. *J. Am. Chem. Soc.* **2011**, *133*, 12608. (n) Gilmore, K.; Alabugin, I. V. *Chem. Rev.* **2011**, *111*, 6513. (o) Stepanov, A. A.; Gornostaev, L. M.; Vasilevsky, S. F.; Arnold, E. V.; Mamatyuk, V. I.; Fadeev, D. S.; Gold, B.; Alabugin, I. V. *J. Org. Chem.* **2011**, *76*, 8737. (r) Roy, S.; Davydova, M. P.; Pal, R.; Gilmore, K.; Tolstikov, G. A.; Vasilevsky, S. F.; Alabugin, I. V. *J. Org. Chem.* **2011**, *76*, 7482. (s) Yang, W.-Y.; Roy, S.; Phrathep, B.; Rengert, Z.; Kenworthy, R.; Zorio, D. A. R.; Alabugin, I. V. *J. Med. Chem.* **2011**, DOI: 10.1021/jm2010282.

(25) (a) Kamijo, S.; Dudley, G. B. *J. Am. Chem. Soc.* **2005**, *127*, 5028. (b) Kamijo, S.; Dudley, G. B. *J. Am. Chem. Soc.* **2006**, *128*, 6499. (c) Tummatorn, J.; Dudley, G. B. *J. Am. Chem. Soc.* **2008**, *130*, 5050.

(d) Jones, D. M.; Lisboa, M. P.; Kamijo, S.; Dudley, G. B. *J. Org. Chem.* **2010**, *75*, 3260. (e) Tummatorn, J.; Dudley, G. B. *Org. Lett.* **2011**, *13*, 158. (f) Tummatorn, J.; Dudley, G. B. *Org. Lett.* **2011**, *13*, 1572.
(26) (a) Dolbier, W. R. Jr.; Koroniak, H.; Houk, K. N.; Sheu, C. *Acc. Chem. Res.* **1996**, *29*, 471. (b) Kirmse, W.; Rondan, N. G.; Houk, K. N. *J. Am. Chem. Soc.* **1984**, *106*, 7989.
(27) Ess, D. H.; Houk, K. N. *J. Phys. Chem. A* **2005**, *109*, 9542.
(28) Miertuš, S.; Scrocco, E.; Tomasi. *J. Chem. Phys.* **1981**, *55*, 117. Cossi, M.; Rega, N.; Scalmani, G.; Barone, V. *J. Comput. Chem.* **2003**, *24*, 669.
(29) Glendening, E. D.; Badenhoop, J. K.; Reed, A. E.; Carpenter, J. E.; Weinhold, F. *NBO 4.0*; Theoretical Chemistry Institute, University of Wisconsin: Madison, WI, 1996.
(30) Reed, A. E.; Curtiss, L. A.; Weinhold, F. *Chem. Rev.* **1988**, *88*, 899.
(31) Previously we have shown that the hyperconjugative energies estimated by second order perturbation and deletion approaches are in excellent agreement with each other: Alabugin, I. V.; Zeidan, T. A. *J. Am. Chem. Soc.* **2002**, *124*, 3175.
(32) (a) Weinhold, F. *Encyclopedia of Computational Chemistry*; Schleyer, P.v.R., Ed.; John Wiley & Sons: New York, 1998; Vol. 3, p 1972. (b) See also: www.chem.wisc.edu/~nbo5.
(33) Reed, A. E.; Weinhold, F. *J. Chem. Phys.* **1985**, *83*, 1736.
(34) (a) Ess, D. H.; Houk, K. N. *J. Am. Chem. Soc.* **2007**, *129*, 10646. (b) Hayden, A. E.; Houk, K. N. *J. Am. Chem. Soc.* **2009**, *131*, 4084. (c) Jones, G. O.; Houk, K. N. *J. Org. Chem.* **2008**, *73*, 1333. (d) Ess, D. H.; Jones, G. O.; Houk, K. N. *Org. Lett.* **2008**, *10*, 1633. (e) Ess, D. H.; Houk, K. N. *J. Am. Chem. Soc.* **2008**, *130*, 10187. (f) Xu, L.; Doubleday, C. E.; Houk, K. N. *Angew. Chem., Int. Ed.* **2009**, *48*, 2746. (g) Lan, Y.; Houk, K. N. *J. Am. Chem. Soc.* **2010**, *132*, 17921. (h) Krenske, E. H.; Houk, K. N.; Holmes, A. B.; Thompson, J. *Tetrahedron Lett.* **2011**, *52*, 2181. (i) Schoenebeck, F.; Ess, D. H.; Jones, G. O.; Houk, K. N. *J. Am. Chem. Soc.* **2009**, *131*, 8121. (j) Krenske, E. H.; Pryor, W. A.; Houk, K. N. *J. Org. Chem.* **2009**, *74*, 5356. (k) Osuna, S.; Houk, K. N. *Chem.—Eur. J.* **2009**, *15*, 13219. (l) Additions to graphene: Cau, Y.; Houk, K. N. *J. Mater. Chem.* **2011**, *21*, 1503. (m) Addition of metals: Ess, D. H. *J. Org. Chem.* **2009**, *74*, 1498. For related activation strain concept, see: (n) Bickelhaupt, F. M.; Ziegler, T.; Schleyer, P. v. R. *Organometallics* **1995**, *14*, 2288. (o) Bickelhaupt, F. M. *J. Comput. Chem.* **1999**, *20*, 114. (p) Velde, G. T.; Bickelhaupt, F. M.; Baerends, E. J.; Guerra, C. F.; Gisbergen, S. J. A. v.; Snijders, J. G.; Ziegler, T. *J. Comput. Chem.* **2001**, *22*, 931. (q) Diefenbach, A.; Bickelhaupt, F. M. *J. Chem. Phys.* **2001**, *115*, 4030. (r) Diefenbach, A.; Bickelhaupt, F. M. *J. Phys. Chem. A* **2004**, *108*, 8460. (s) Diefenbach, A.; Bickelhaupt, F. M. *J. Organomet. Chem.* **2005**, *690*, 2191. (t) Diefenbach, A.; de Jong, G. T.; Bickelhaupt, F. M. *Mol. Phys.* **2005**, *103*, 995. (u) Diefenbach, A.; de Jong, G. T.; Bickelhaupt, F. M. *J. Chem. Theory Comput.* **2005**, *1*, 286. (v) van Stralen, J. N. P.; Bickelhaupt, F. M. *Organometallics* **2006**, *25*, 4260. (w) de Jong, G. T.; Visser, R.; Bickelhaupt, F. M. *J. Organomet. Chem.* **2006**, *691*, 4341. (x) de Jong, G. T.; Bickelhaupt, F. M. *Chem. Phys. Chem.* **2007**, *8*, 1170. (y) de Jong, G. T.; Bickelhaupt, F. M. *J. Chem. Theory Comput.* **2007**, *3*, 514.
(35) Alabugin, I. V.; Zeidan, T. A. *J. Am. Chem. Soc.* **2002**, *124*, 3175.
(36) (a) Strozier, R. W.; Caramella, P.; Houk, K. N. *J. Am. Chem. Soc.* **1979**, *101*, 1340. (b) Houk, K. N.; Strozier, R. W.; Rozeboom, M. D.; Nagaze, S. *J. Am. Chem. Soc.* **1982**, *104*, 323.
(37) Ng, L.; Jordan, K. D.; Krebs, A.; Ruger, W. *J. Am. Chem. Soc.* **1982**, *104*, 7414.
(38) (a) Ronan, N. G.; Domelsmith, L. N.; Houk, K. N.; Bowne, A. T.; Levin, R. H. *Tetrahedron Lett.* **1979**, *35*, 3237. (b) Recent synthetic applications: Bajracharya, G.; Daugulis, O. *Org. Lett.* **2008**, *10*, 4625. (c) Truong, T.; Daugulis, O. *J. Am. Chem. Soc.* **2011**, *133*, 4243.
(39) Interestingly, even though the two methyl groups are in a staggered conformation in 2-butyne, they adopt an eclipsed conformation in the cycloaddition TS. This conformational change positions the σ^*(C−H) orbitals antiperiplanar to the bent in-plane alkyne π-orbitals and the incipient C−N bonds, suggesting the increased importance of hyperconjugation in the TS.
(40) Alabugin, I. V.; Manoharan, M.; Peabody, S.; Weinhold, F. *J. Am. Chem. Soc.* **2003**, *125*, 5973.
(41) Pross, A.; Shaik, S. S. *Acc. Chem. Res.* **1983**, *16*, 363.
(42) One has to keep in mind, however, that π-acceptors should also accelerate nucleophilic addition to the triple bond and thus may increase the importance of side reactions.
(43) Hamper, B. C. *Org. Synth.* **1992**, *70*, 246.
(44) (a) Li, Z.; Seo, T. S.; Ju, J. *Tetrahedron Lett.* **2004**, *45*, 3143. (b) Guerin, D. J.; Miller, S. J. *J. Am. Chem. Soc.* **2002**, *124*, 2134−2136. (c) Fu, X.; Albermann, C.; Jiang, J.; Liao, J.; Zhang, C.; Thorson, J. S. *Nat. Biotechnol.* **2003**, *21*, 1467.
(45) Reaction of diethyl but-2-ynedioate, ethyl 2-butynoate, and methyl propiolate (0.25 M) with ethyl 5-azidovalerate in water was reported to proceed to completion at ambient temperatures in 6−12 h: Li, Z.; Seo, T. S.; Ju, J. *Tetrahedron Lett.* **2004**, *45*, 3143. On the other hand, the reaction of dimethyl but-2-ynedioate, ethyl 2-butynoate, and methyl propiolate with (*R*)-1-(3-azido-3-cyclohexylpropanoyl)pyrrolidin-2-one in toluene (130°C for 24−48 h) (Guerin, D. J.; Miller, S. J. *J. Am. Chem. Soc.* **2002**, *124*, 2134) was much slower and more consistent with reactivity observed by us for alkyne **1** in acetonitrile. These observations suggest that water imposes significant acceleration effect on this transformation.
(46) van Berkel, S. S.; Dirks, J.; Debets, M. F.; van Delft, F. L.; Cornelissen, J. J. L. M.; Nolte, R. J. M.; Rutjes, F. P. J. T. *ChemBioChem.* **2007**, *8*, 1504.
(47) Campbell-Verduyn, L.; Elsinga, P. H.; Mirfeizi, L.; Dierckx, R. A.; Feringa, B. L. *Org. Biomol. Chem.* **2008**, *6*, 3461.
(48) Chu, L.; Qing, F. *J. Am. Chem. Soc.* **2010**, *132*, 7262.